S-MODE Bio-optical Data (V3) Report for IOP-1

Sarah Lang, Melissa Omand, Roger Patrick Kelly

This data report describes the steps taken to quality-control, calibrate bio-optical parameters, and develop biogeochemical proxies from the bio-optical measurements collected during the S-MODE IOP-1 campaign. The S-MODE study area extended about 200 km off the coast of San Francisco (Fig. 1), and the data described in this report were collected between October 8 and October 31, 2023. In this report, we outline our preliminary methods for calibrating bio-optical instruments on the underway system installed on the R/V Bold Horizon, EcoCTD, 4 Saildrones, and 4 Seagliders used during the Fall 2022 IOP-1 Campaign. We also describe our methods for creating optical based proxies of chlorophyll concentrations (Chl; µg/l or $mg/m^{3)}$ and particulate organic carbon (POC) molarity (µmol/L).

Table of contents

Section 1: Data Overview

** Note this list includes only the instruments used for the analysis contained in this report.

RV *Bold Horizon*:

- Bottle datasets for POC [µmol/L] (n=172), PON [µmol/L] (n=172), Chl [mg m^{-3}] (n=199), and HPLC (n=142) were collected from the flow-through system and 17 CTD casts (POC and PON: n = 71; chl: n = 106; HPLC: n = 106). These data are available on PO.DAAC (doi: 10.5067/SMODE-RVBOT). See section 2 for more information

- Flow-through optical data

The flow-through optical system contained a de-bubbler, TSG (thermosalinograph; Seabird Scientific SBE45), filter switch, ACS (hyperspectral absorption and beam attenuation; Seabird Scientific ACS-111), WET Labs C-Star (beam transmittance at one visible wavelength with a 25 cm pathlength; Sea-bird Scientific CST-447PR), WET Labs chlorophyll-fluorometer (Seabird Scientific WS3S1081P), CDOM-fluorometer (Seapoint Sensors, inc. SUVF6245), and WET Labs BB3 (optical backscatter at three visible wavelengths; Seabird Scientific BB3-1052).

Instruments sampled nearly continuously. In default mode, the system sampled filtered seawater (to measure the optical properties of water + dissolved constituents) during the first 10 minutes of every hour, and automatically switched to total seawater. This sampling routine allows for robust calibration of the optical properties of the particulates (parameters of interest), as instrument error (eg. drift) gets subtracted out (particulate = total – filtered) (Slade et al., 2010). This sampling routine was modified when crossing dynamical features of interests or during airborne overpasses.

The instruments on the flow through system were cleaned every 5 - 8 days, and the mesh filter to filter out large zooplankton and other particles was cleaned nearly every day (captured a lot of gelatinous material). The flow rate through the system was around 2.5 L/min (3 L/min is ideal, but could not be achieved due to system constraints).

Due to technical errors, there are data missing from the following three instruments between Oct. 18th - 24th: chlorophyll fluorometer, C-Star, and SUVF. However, duplicate measurements from the C-Star were taken by the ACS, and our chlorophyll-a proxy came from the ACS and

relationships between the ACS and chlorophyll fluorometer. Therefore, there are no gaps in continuous chlorophyll-a (chl) and particulate organic carbon (POC) proxies from the ship.

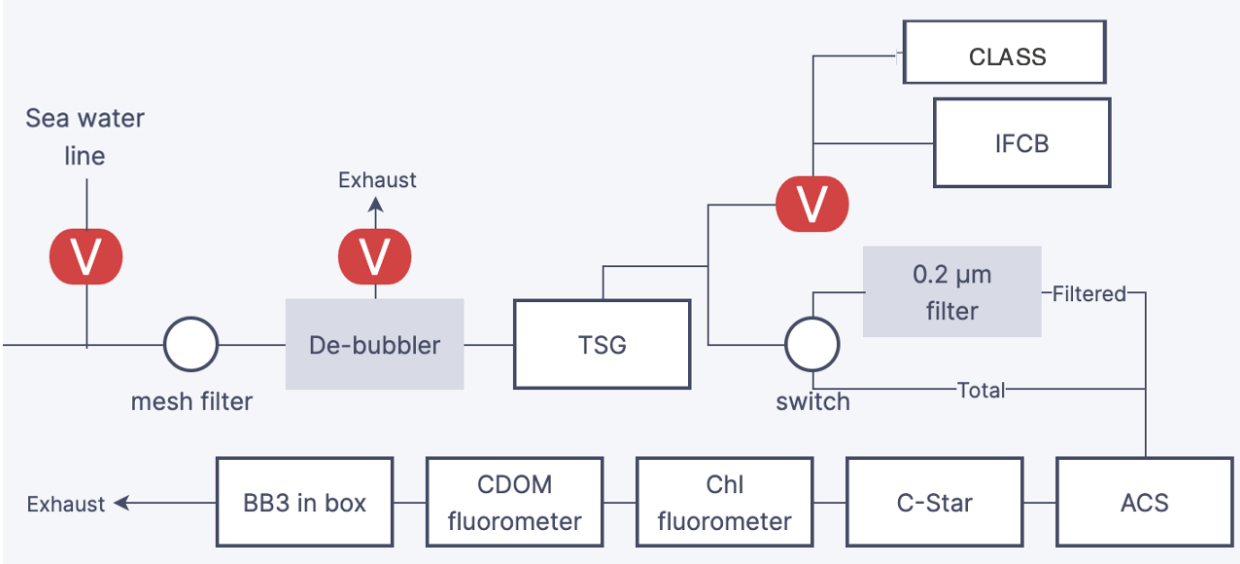

Figure 1. Schematic of underway optical system connected to uncontaminated science seawater line. Seawater traveled through mesh to filter out large zooplankton and other large particles. De-bubbler prevented bubbles from contaminating optical measurements. Seawater is then measured by the TSG, after which the line splits into two branches: the IFCB/CLASS line and the flow-through optics line (controlled by automatic switch, white circle). Red V's denote location of valves.

- EcoCTD vertical profiler

The EcoCTD is an underway vertical profiler capturing simultaneous hydrographic and biological data at submesoscale spatiotemporal resolutions (Dever et al., 2020), allowing us to resolve the vertical structure of sampled fronts. The EcoCTD contained an ECO Puck from Seabird Scientific, measuring optical backscatter at 470 nm and 700 nm at a 117˚ scattering angle and chlorophyll-fluorescence.

- RBR Maestro on CTD-Rosette

The RBR Maestro is a battery powered CTD that contains bio-optics. The RBR Maestro was strapped to the CTD-Rosette for all 17 CTD casts during IOP-1. The instrument measured conductivity, temperature, pressure, dissolved oxygen, backscatter at 700 nm, chlorophyll-fluorescence, CDOM (colored dissolved organic matter) fluorescence, and transmittance. Data available will also contain derived variables such as calibrated chlorophyll, particulate organic carbon, depth, potential density, conservative temperature, absolute salinity, and beam attenuation.

Table 1: Cast numbers and times. Calibration casts starred. Cast with bad quality bio-optical data in red.

1) 14-Oct-2022 17:52
2) 14-Oct-2022 20:54
3) 16-Oct-2022 03:22 ***
4) 19-Oct-2022 09:22 ***
5) 19-Oct-2022 10:22 ***
6) 19-Oct-2022 11:48 ***
7) 19-Oct-2022 12:38 ***
8) 19-Oct-2022 13:27 ***
9) 21-Oct-2022 07:06
10) 25-Oct-2022 08:34 ***
11) 25-Oct-2022 09:17 ***
12) 25-Oct-2022 10:00
13) 25-Oct-2022 10:43 ***
14) 25-Oct-2022 11:26 ***
15) 27-Oct-2022 23:54
15a) 28-Oct-2022 00:50
16) 28-Oct-2022 21:00
17) 28-Oct-2022 23:44:07 ***

Autonomous vehicles

- Saildrones

  WETLabs BBFL2W ECO Triplets were integrated onto 4 Saildrones, measuring chlorophyll fluorescence (excitation at 470 nm, emission at 695 nm) and optical backscatter at 650 nm.

- Seagliders

  Wetlabs ECO-BB2F measuring chlorophyll-fluorescence and optical backscatter at 2 wavelengths (470 nm and 700 nm) at an 124˚ scattering angle.

- Wavegliders

One Waveglider (WHOI43) had an RBR Concerto with a bio-optical package including chlorophyll-fluorescence, backscatter at 700 nm, and beam transmittance.

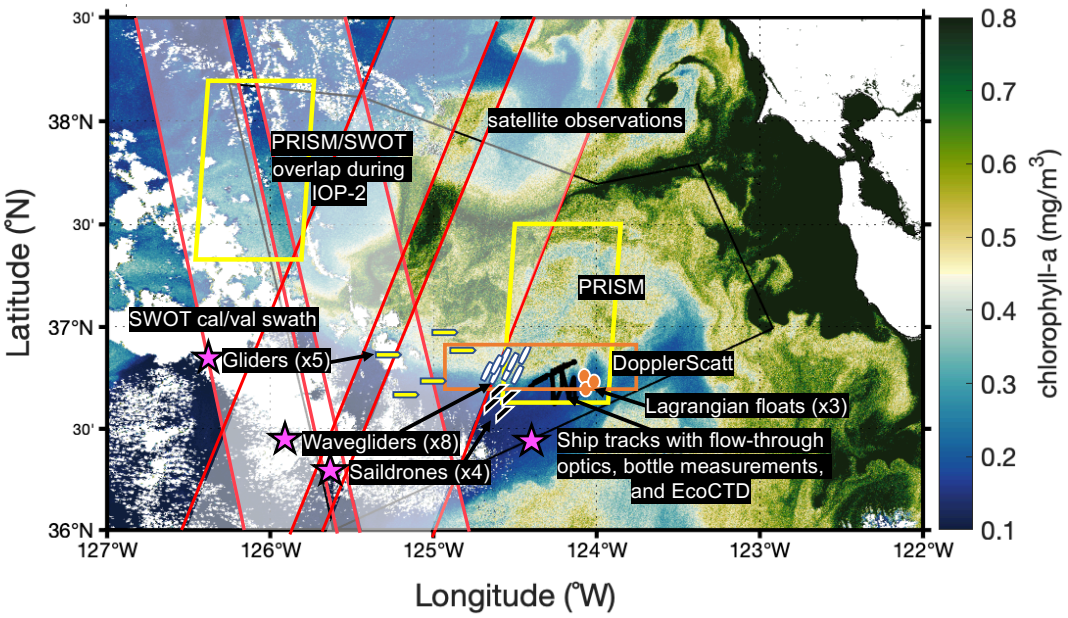

Figure 2: Multi-platform, multi-scale approach used to characterize the mesoscale and submesoscale. Map of Sentinel-3 OLCI chlorophyll-a (300m resolution) on Oct. 26 with SWOT calibration/validation swath overlain (red and white), PRISM coverage (yellow), DopplerScatt coverage (orange), ship tracks (black), Wavegliders (white and blue icons), Lagrangian floats (orange icons), Saildrones (black and white icons), and gliders (yellow icons). Assets included in this report denoted by pink stars.

Section 2: Ground-truth data: Bottle measurement procedures

2.1 Chlorophyll extractions (on ship)

Samples were collected in pre-tared 500 ml LDPE bottles after gently rinsing with sample water 3 times. The samples were then filtered gently through Whatman GF/F filters under low vacuum (5-10 in Hg). After the sample had passed through the filter, the bottle and filter funnels were rinsed 3 times with GF/F filtered seawater. In some cases, filters were subsampled for HPLC pigment analysis using a 10mm diagram arch punch. Sample filters were then placed in 10ml glass cuvette and stored in a dark refrigerator until sampling was complete, at which point 6 ml of 90% acetone / 10% water was added to extract the chlorophyll pigments.

After extracting for 24 hours, the samples were analyzed on a Turner A10 fluorometer. The fluorometer had been calibrated prior to the cruise using a known set of chlorophyll standards and verified during the cruise pre- and post- measurement with a fluorescence cuvette standard. Prior to measurement, samples were vortexed for 5 seconds to remove extracted pigments from the GF/F filter, which was then taken out of the vial. The vial was wiped to remove any residues from the glass and measured for fluorescence in triplicate. Samples that were over the limit were diluted to 3% with 90% acetone and re-analyzed. After completing a batch, phaeopigments were

extracted by adding a drop of 10% hydrochloric acid each sample and vortexing it for 5 seconds. After standing for 15 minutes, samples were reanalyzed on the Turner A10.

2.2 Particulate organic carbon and nitrogen (URI)

Samples were collected in graduated 4L LDPE bottles after gently rinsing with sample water 3 times. Bottles were filled to 2-4L, based on apparent particle loading estimated from the science seawater system flow-through transmissometer readout. The samples were then filtered gently through pre-combusted Whatman GF/F filters under low vacuum (5-10 in Hg) by inverting the 4L bottle into a filter funnel. In cases where particle loading was substantial, samples that were not completely filtered after ~3 hours were stopped and the remaining sample volume recorded using a 250 ml graduated cylinder. This volume was subtracted from the initial volume to correct for the unfiltered fraction. After the sample had passed through the filter, the bottle and filter funnels were rinsed 3 times with GF/F filtered seawater. Samples were placed in labeled polycarbonate petri dishes and stored frozen until analysis at the University of Rhode Island. Filter funnels and forceps were cleaned with acetone and kim wipes between samples.

Prior to analysis at the University of Rhode Island, samples were dried overnight at 60℃ in a drying oven. They were then subsampled for POC by cutting a visually representative wedge using scissors and forceps cleaned with ethanol. The POC wedge and archive components were then weighed on an analytical balance to determine their relative fraction of the whole filter (15-50% for POC, based on particle loading). The POC subsamples were then exposed to hydrochloric acid fumes in an acid desiccator for 24 hours, while the archive piece was returned to frozen storage. The POC subsamples were then dried again at 60˚C overnight and packed into 5x9 mm ultra-clean tin capsules and stored in 96-well plates. The POC samples were then analyzed for carbon and nitrogen using a Costech 4010 Elemental Analyzer using aminocaproic acid as the standard.

Section 3: Calibrations

3.1 Optical measurements and initial corrections

For all flow-through measurements except CDOM fluorescence, filtered data (first 10 minutes of every hour) was subtracted from total data (remaining 50 minutes) after interpolating between the median of each filter event. This isolated measurements of the particulate fraction of the water.

All optics-bottle match-ups for proxies were done on 1-minute binned optical data to match the approximate time it takes to collect a water sample from the flow-through system.

3.1.1 Flow-through beam attenuation

Factory calibrations, as set by SeaBird Scientific, were applied to raw transmittance values (Eq. 1).

$$Tr = (V_{sig} - V_{dark}) / (V_{ref} - V_{dark}) \quad (1)$$

Where V_{sig} is the raw transmittance measured by the instrument, V_{dark} (V_{dark} = 0.058) is the output with the beam blocked (offset), and V_{ref} is output in clean water (V_{ref} = 4.724).

Transmittance was converted to beam attenuation coefficient (c_p, m^{-1}; Eq. 2) with a conversion set by the manufacturer.

$$c_p = \frac{-1}{0.25} ln(Tr) \quad (2)$$

where 0.25 is the pathlength of the instrument in meters, and *Tr* is the transmittance (dimensionless).

3.1.2 Flow-through chlorophyll-fluorescence

Chlorophyll fluorescence from the underway [volts] was binned in 1 minute intervals and left in raw units until intercalibrated with ACS-derived chlorophyll to yield calibrated standard units [µg/L] (section 3.3.1).

3.1.3 Flow-through ACS absorption line height at 676 nm

Residual temperature and salinity corrections were applied to all ACS particulate absorption (ap) and particulate beam attenuation (cp) as in Slade et al., 2010. ACS data was also unsmoothed, following the methods of Chase et al., 2013, to avoid the smoothing of spectral features. Any negative values were deleted.

Further quality control was conducted following methods from the University of Maine's Maine In-situ Sound & Color Lab (MISC) at https://github.com/OceanOptics/InLineAnalysis: Unrealistic ap and cp spectra were deleted based on the following criteria: if the first derivate of ap over the wavelengths 460 and 640 nm was larger than 0.2 times ap at 450 nm, the second derivative of ap over the wavelengths 460 and 640 nm were larger than 0.006, there were 4 consecutive positive first derivatives of ap over wavelengths 485 and 570 nm, or there were 5 consecutive positive first derivatives of cp over wavelengths 485 and 570 nm.

Data from October 15 was flagged. The absorption and beam attenuation spectra may have been affected by bubbles.

Absorption line height, a measure of the pigment absorption peak in the red associated with chlorophyll-a, has been shown to be a robust proxy for chlorophyll-a unaffected by non-photochemical quenching (Roseler & Barnard 2013). The equations are as follows:

$$a_{BL}(\lambda_{ref}) = \frac{a(715) - a(650)}{715 - 650} * (\lambda_{ref} - 650) + a \quad (3)$$

$$a_{LH}(676)(m^{-1}) = a(676) - a_{BL}(676) \quad (4)$$

With numbers denoting wavelengths in nm, λ_{ref} as the reference wavelength of 676 nm, a_{BL} as the absorption value of the baseline between 650 nm and 715 nm, a(715) as the absorption at 715 nm, a(650) as the absorption at 650 nm, and $a_{LH}(676)$ as the absorption line height at 676 nm (proxy of interest).

We expect a linear fit between $a_{LH}(676)$ and extracted chlorophyll analyzed from near surface seawater samples from Roseler & Barnard 2013.

3.1.4 Flow-through ACS c_p at 657 nm

Corrections were applied to ACS data as in Section 3.1.3. $C_p(657)$ nm was chosen as the POC proxy to match the wavelength of the WET Labs C-Star.

3.1.5 Flow-through backscatter at 476 nm, 532 nm, and 651 nm

The following calibration coefficients were applied to raw counts of bb(476), bb(532), and bb(651) before subtracting filtrate bb from total bb to yield particulate bb: 1.20e-5 $m^{-1}sr^{-1}$, 1.23e-5 $m^{-1}sr^{-1}$, and 4.88e-6 $m^{-1}sr^{-1}$. Measurements were multiplied by a correction factor of $2\pi\chi$ (χ = 1.076 for volume scattering angle = 117˚) as in Boss & Pegau 2001.

3.1.6 Flow-through CDOM fluorescence

CDOM fluorescence had no corrections applied. It can be used as a relative measure of CDOM.

3.1.7 EcoCTD chlorophyll-fluorescence and optical backscatter

Chlorophyll fluorescence (counts) were left in raw units until calibrated with bottle samples from the CTD-Rosette to yield calibrated standard units [µg/L].

Optical backscatter at 470 nm (bb(470)) from the EcoCTD [counts] was converted to standard units (m^{-1} sr^{-1}) with factory calibrations provided by WETLabs (Eq. 5):

$$bb(470)\ [m^{-1}sr^{-1}] = 0.0143\ [m^{-1}sr^{-1}]/count * (Output - 79)\ counts \quad (5)$$

where 48 denotes the dark counts. Optical backscatter at 700 nm (bb(700)) from the EcoCTD [counts] was converted to standard units (m^{-1} sr^{-1}) with factory calibrations provided by WETLabs (Eq. 6):

$$bb(700)\ [m^{-1}sr^{-1}] = 0.002\ [m^{-1}sr^{-1}]/count * (Output - 100)\ counts \quad (6)$$

Temperature and salinity corrections, as well as a correction for the volume scattering angle, were then applied to optical backscatter measurements as in Zhang et al. 2009. We used simultaneous *in situ* temperature and conductivity (converted to practical salinity via the Gibbs

Seawater (GSW) Oceanographic Toolbox; McDougall & Barker 2011) recorded by the same platform for corrections. Measurements were multiplied by a correction factor of $2\pi\chi$ ($\chi = 1.076$ for volume scattering angle = 117°) as in Boss & Pegau 2001.

After applying manufacturer's calibrations to EcoCTD backscatter, backscatter values were 3 orders of magnitude too high. We used the calibration casts to correct EcoCTD bb(700) (our proxy for POC) relative to bb(700) from the RBR Maestro (manufacturer calibrations, standard temperature, salinity, and scattering angle corrections applied to Maestro bb(700) data before comparison) (Figs. 3,4,5).

Casts 3, 4, 5, 6, and 8 had deep bb(700) values that were too high because the EcoPuck sensor was facing the rosette (Fig. 3). These casts were corrected by applying an offset found by subtracting the median of deep bb(700) (median of values between 180 m – 200 m) of the unaffected casts from the median of deep bb(700) of each of these elevated casts (Fig. 4).

A 5 meter median filter was applied to bb(700) from both the RBR Maestro and the EcoCTD, and a linear fit between RBR bb(700) and EcoCTD bb(700) was used to correct EcoCTD bb(700) ($R_{adj}^2 = 92.1\%$, $F_{1,1474} = 17100$, $P < 0.001$; Fig. 5, Eq. 7).

$$[\text{corrected bb(700)}\ \ (\text{m}^{-1}\text{sr}^{-1})]] = 0.00196\ [\text{uncorrected bb(700)}\ (\text{m}^{-1}\text{sr}^{-1})] + 0.000533 \quad (7)$$

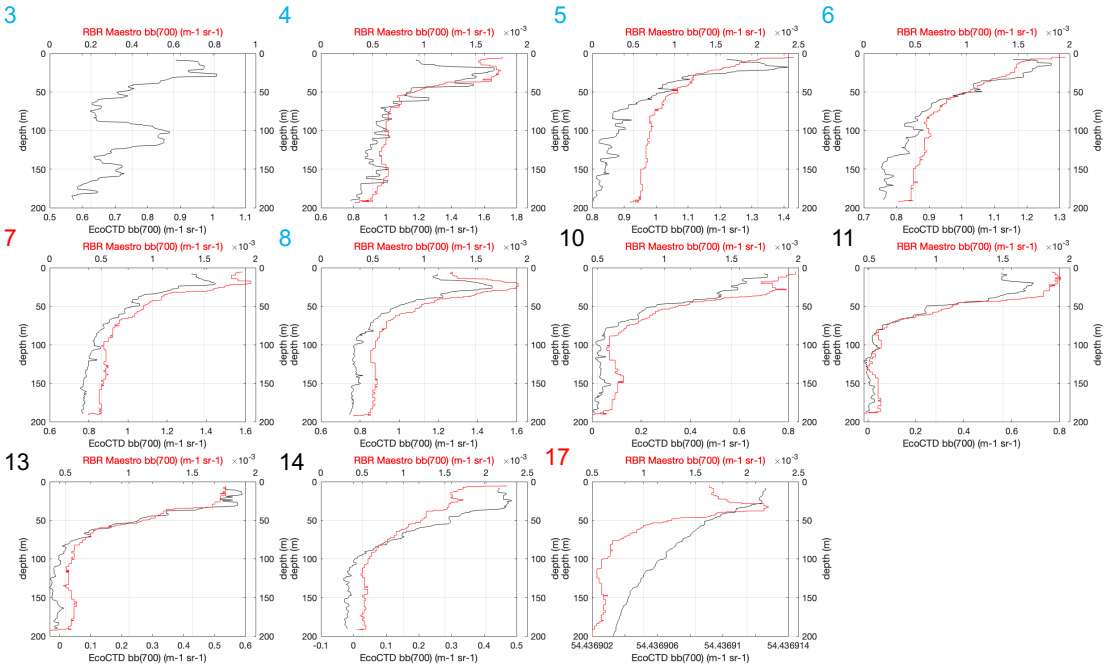

Figure 3: Depth plotted against RBR Maestro bb(700) with manufacturer calibrations applied shown in red (top x-axis). Depth plotted against EcoCTD bb(700) with manufacturer calibrations applied shown in black (bottom x-axis). Numbers denote cast numbers associated with calibration casts listed in Table 1. Blue numbers denote casts when the EcoPuck was facing the Rosette, resulting in elevated bb(700) values. These casts were corrected by subtracting an offset.

Red casts (i.e. 7, 17) were excluded from calibrations due to poor data quality as explained in 3.2.3.

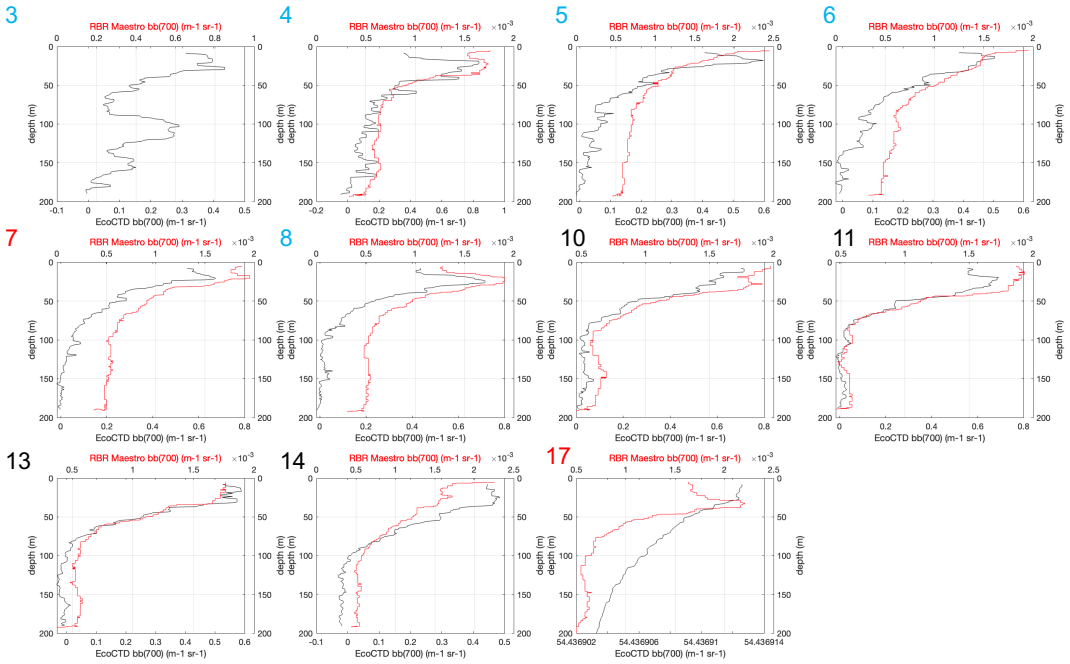

Figure 4: Depth plotted against RBR Maestro bb(700) with manufacturer calibrations applied shown in red (top x-axis). Depth plotted against EcoCTD bb(700) with manufacturer calibrations applied shown in black (bottom x-axis). Numbers denote cast numbers as in Fig. 3, and number colors denote data quality and corrections as in Fig. 3.

Cast 17 was excluded because bb(700) measurements were 2 orders of magnitude higher than the rest of the casts.

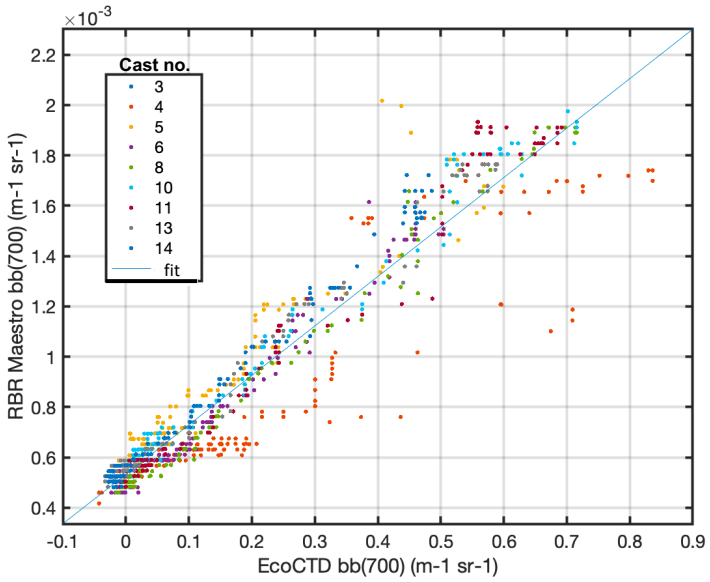

Figure 5: RBR Maestro bb(700) (y-axis) plotted against EcoCTD bb(700) for each calibration cast. Linear fit used to correct data in blue.

3.1.8 Seaglider optical backscatter at 470 nm and 700 nm

Seaglider bb(470) and bb(700) underwent standard temperature, salinity, and scattering corrections as in 3.1.7.

3.1.9 Saildrone optical backscatter at 650 nm

Saildrone data was binned in 1 minute intervals. Standard corrections (temperature, salinity, volume scattering angle, $2\pi\chi$ factor, (χ = 1.1 for volume scattering angle = 124˚) were applied as in Section 3.1.7.

3.1.10 Waveglider optical backscatter at 700 nm

Waveglider optical measurements were left at the original resolution of the RBR Concerto (5 second intervals). Factory calibrations were unavailable so the same manufacturer calibrations as the bb(700) on the RBR Maestro on the CTD (same sensor type, bb(700) [$m^{-1}sr^{-1}$] = 3.07e-6 [$m^{-1}sr^{-1}$]/count $*$ (Output – 48)). Standard corrections (temperature, salinity, volume scattering angle, $2\pi\chi$ factor, (χ = 1.1 for volume scattering angle = 124˚) were applied as in Section 3.1.7.

3.1.11 Waveglider beam attenuation at 650 nm

Factory calibrations, as set by SeaBird Scientific, were applied to raw transmittance values as in 3.1.1 (Eq. 1), with different coefficient values (V_{dark} = 0.0.002, V_{ref} = 4.699). Transmittance (Tr) was converted to beam attenuation coefficient (c_p, m^{-1}; Eq. 2) with a conversion set by the manufacturer as in 3.1.1. Resulting values were unrealistic, but we performed our own calibrations with underway data (section 3.3.6). We advise against using beam attenuation data as is, and instead using calibrated POC from cp (as outlined in section 3.3.6).

3.2 Primary optical proxies (directly from bottle measurements)

3.2.1 Chlorophyll-a (Chl) proxies from flow-through absorption line height and chlorophyll-fluorescence

Absorption line height at 676 nm, calculated from ACS absorption curves (described in section 3.1.3), were binned in 1 minute intervals to match the approximate time it takes to collect a corresponding bottle sample.

Chlorophyll concentrations remained low in the study region for the duration of the cruise. 149 out of 163 bottle samples for match-up were below 1 µg/L. To avoid overweighting high values, we fit a line in log space between chlorophyll concentrations from bottle seawater samples

(described in section 2.1) and absorption line height calculated by ACS-absorption measured in-line, forcing the slope to 1. We then converted this back to linear space.

We chose to exclude 3 outliers on 10/13 taken closer to shore. 3 other bottle measurements taken close to shore were also excluded because corresponding ACS-absorption values did not pass quality control (described in 3.1.3).

The fit was significant (R_{adj}^2 = 75.9%, RMSE = 0.16 µg/L, MAPE = 22%, N = 154). This fit yielded an empirical formula for absorption line height (alh; m^{-1}) to calibrated chlorophyll concentrations (µg/L) (Eq. 8, Fig. 7).

$$[\text{calibrated chlorophyll (µg/L)}] = 10^{1.74}[\text{alh}] \qquad (8)$$

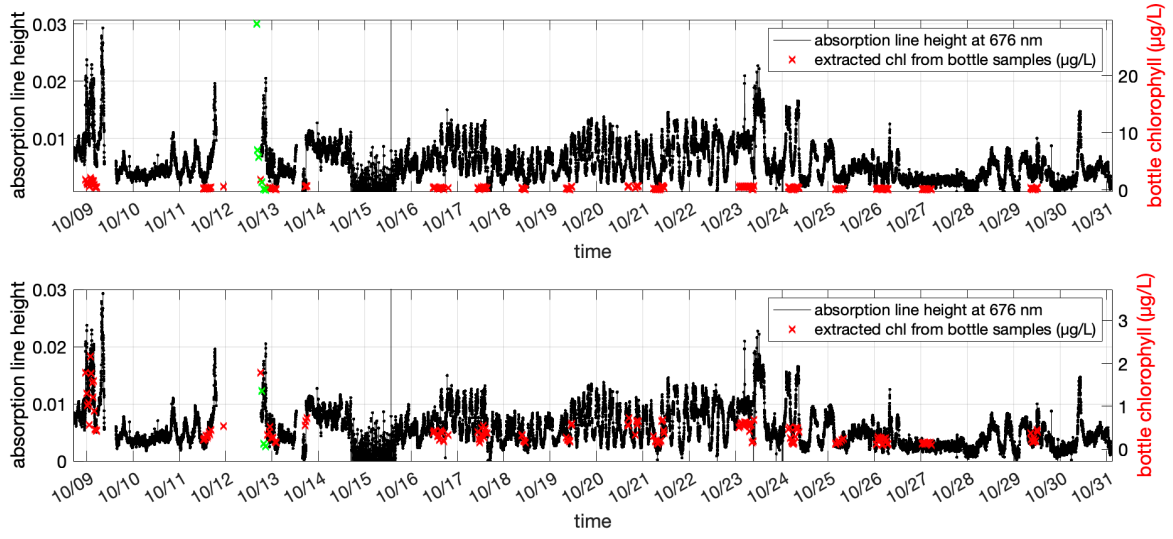

Fig. 6: Absorption line height (left y-axis, black) and bottle chlorophyll (right y-axis, red) plotted against time for all bottle samples (top) and bottles samples less than 3 µg/L (bottom). Excluded match-ups denoted by green x's.

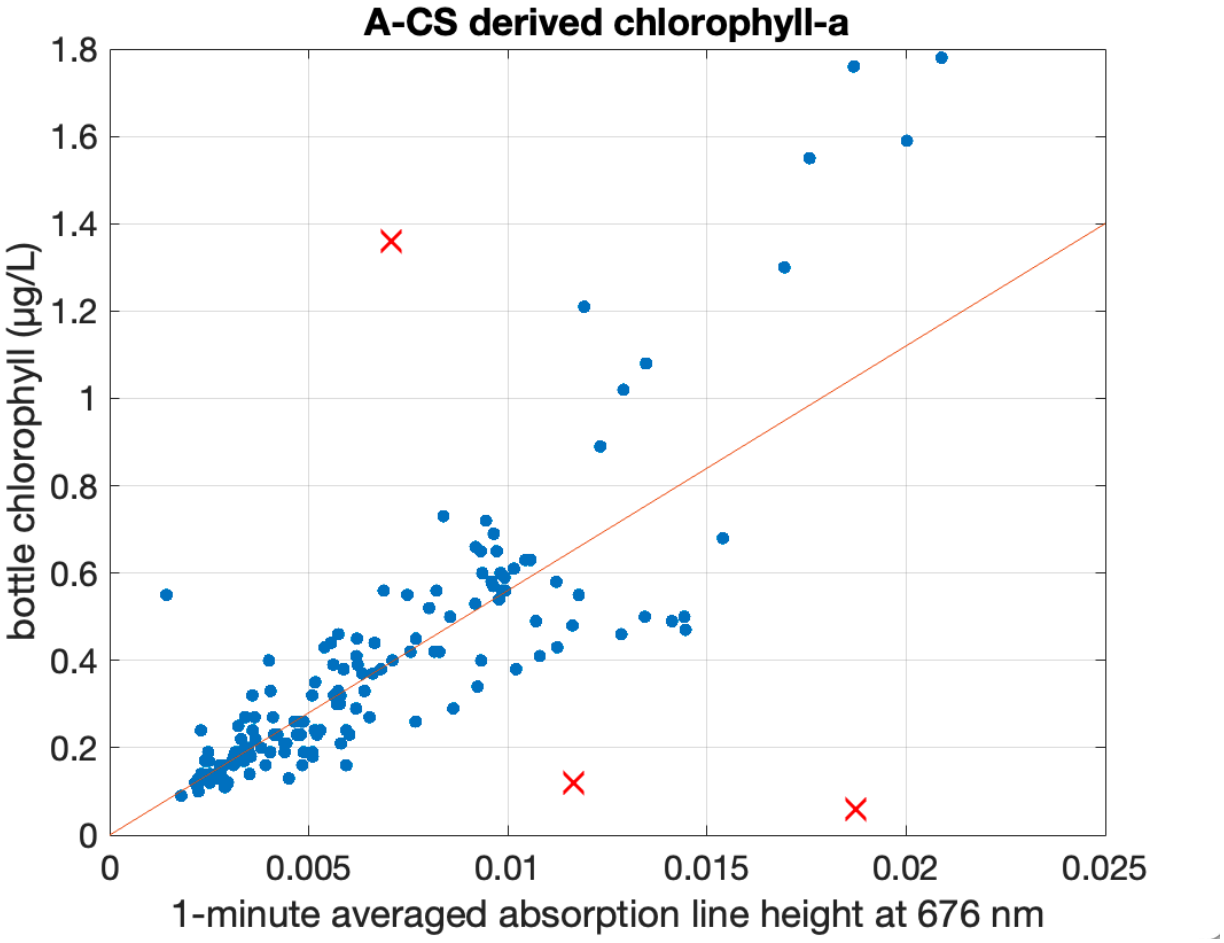

Figure 7: Bottle chlorophyll (y-axis) plotted against 1-minute averaged absorption line height at 676 nm from the ACS (x-axis). Fit from Eq. 7 in red. Outliers denoted by red x's.

3.2.2 Particulate organic carbon (POC) proxy from ACS beam attenuation

2 outliers were excluded from the fit because they were more than 8 standard deviations away from the fit excluding them.

We fit a line in log space between POC concentrations from seawater samples and ACS beam attenuation at 657 nm in-line, forcing the slope to 1 as in 3.2.1.

ACS beam attenuation (cp) at 657 nm (m^{-1}; Fig. 8) was a strong predictor for POC (µmol/L; R_{adj}^2 = 64.4%, RMSE=1.21 µmol/L, MAPE= 14.5%, N=146, Fig. 9, Eq. 9).

$$[\text{calibrated POC } (\mu\text{mol/L})] = 10^{1.58}[\text{ACS cp}(657)] \qquad (9)$$

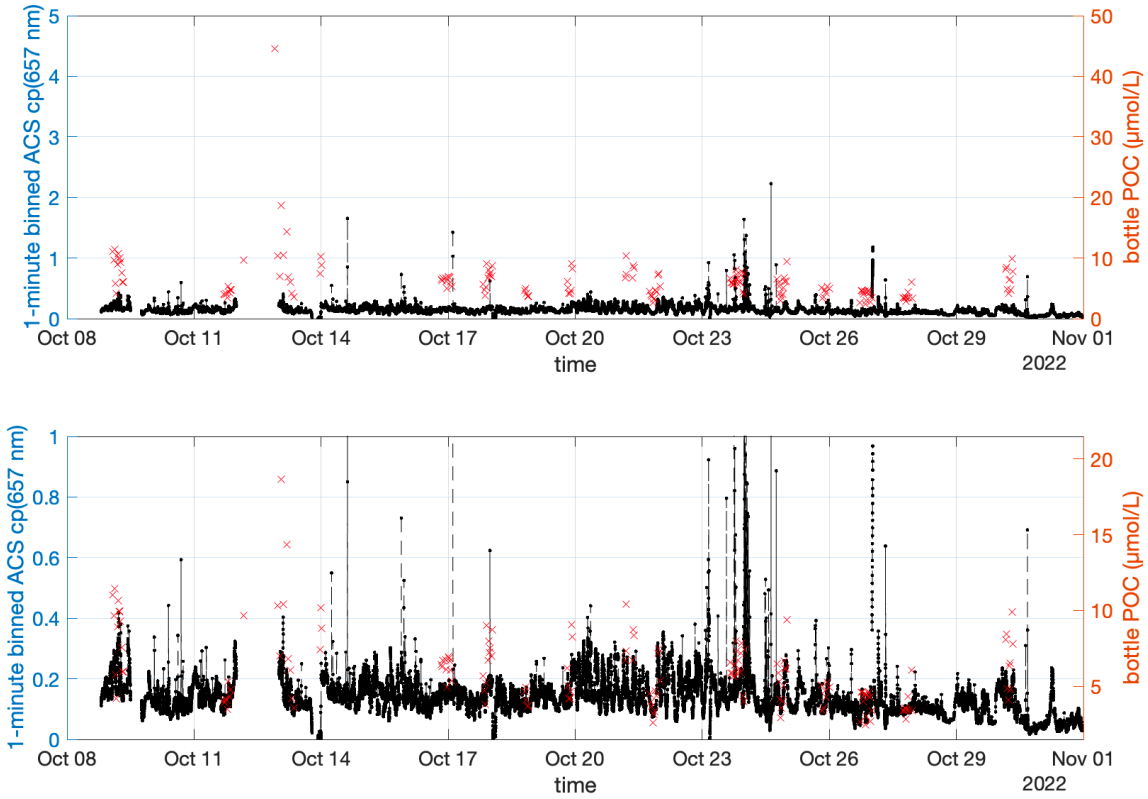

Fig. 8: 1-minute binned ACS cp(657) (left y-axis, black) and bottle chlorophyll (right y-axis, red) plotted against time for all bottle samples (top) and bottles samples less than 20 µg/L (bottom).

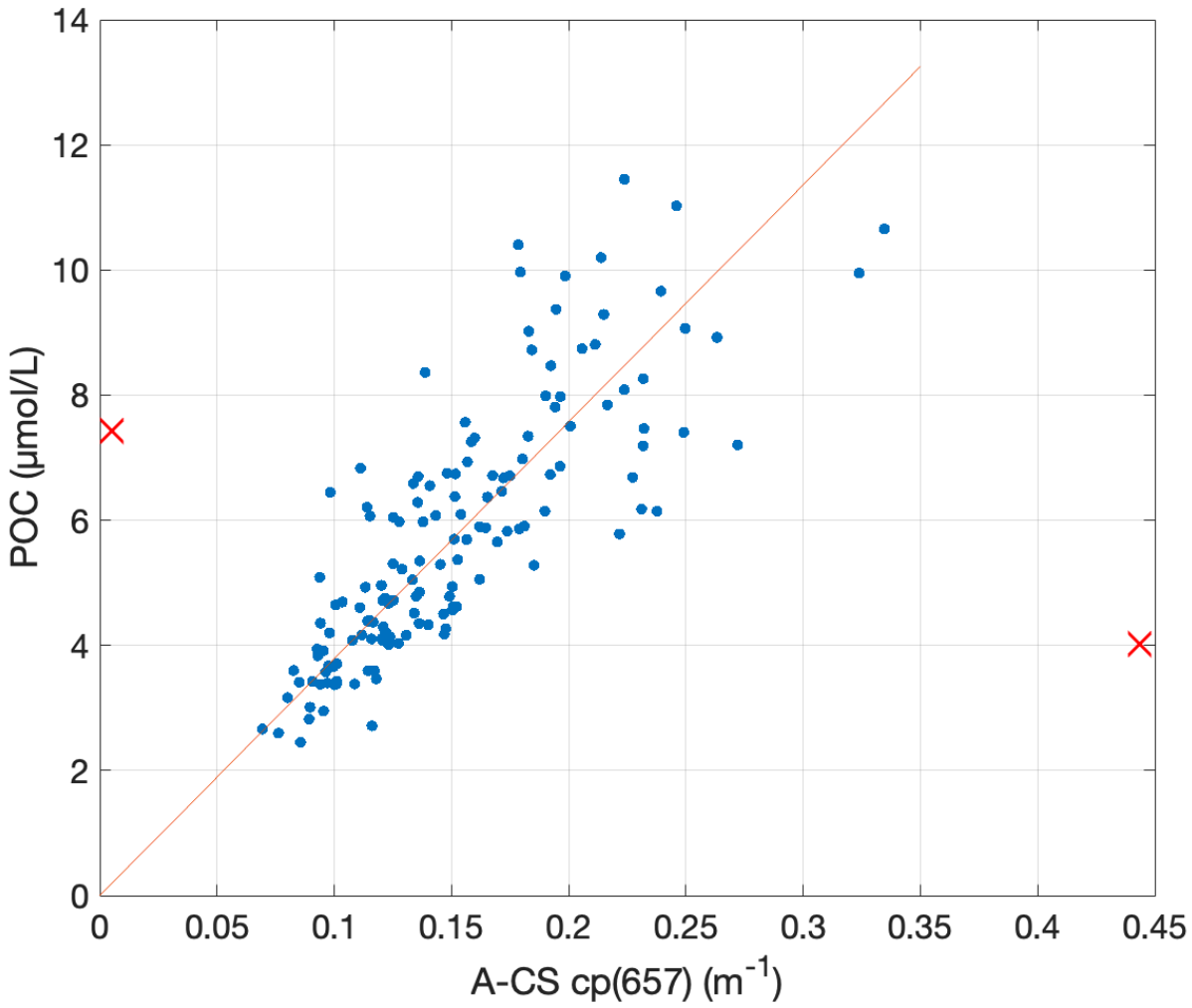

Figure 9: Bottle POC (y-axis) plotted against 1-minute averaged beam attenuation at 657 nm from the ACS (x-axis). Fit from Eq. X in red. Outliers denoted by red x's.

3.2.3 Calibrated Chl-Fl from EcoCTD

There were 11 calibration casts with the EcoCTD strapped on the CTD-Rosette (Table 1). A line was fit between uncalibrated EcoCTD chl-fl and chlorophyll analyzed from Niskin bottle seawater samples ($R_{adj}^2 = 75.4\%$, $F_{1,50} = 157$, $P < 0.001$; Fig. 11, Eq. 10). Data was matched up by depth.

We also explored a separate fit using a similar fitting procedure as in 3.2.1 and 3.2.2 to give higher weight to lower values (after subtracting a dark count of 53, minimum EcoCTD value on rosette, red line in Fig. 11). However, vertical profiles capture a larger range in chlorophyll concentrations than surface sampling, so we opted for the linear fit (blue line in Fig. 11).

Match-ups from cast 17 were outliers and were removed from the calibration curve (x's in Fig. 11, left). EcoCTD chl-fl values from this cast were anomalously high, despite bottle chlorophyll values being within range of samples from the other casts (Fig. 10).

$$[\text{chl}] = 0.0085\ (\text{chl-fl}) - 0.04 \qquad (10)$$

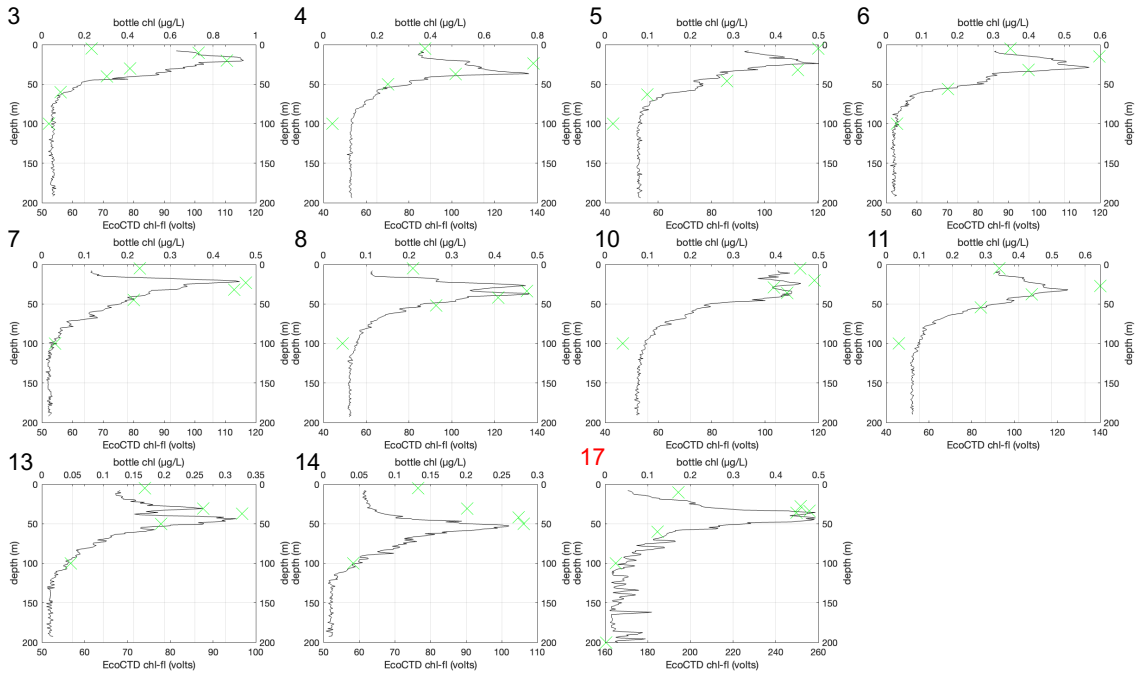

Figure 10: Depth plotted against bottle chlorophyll-a (top x-axis) in green. Depth plotted against EcoCTD chl-fl (bottom x-axis) in black.

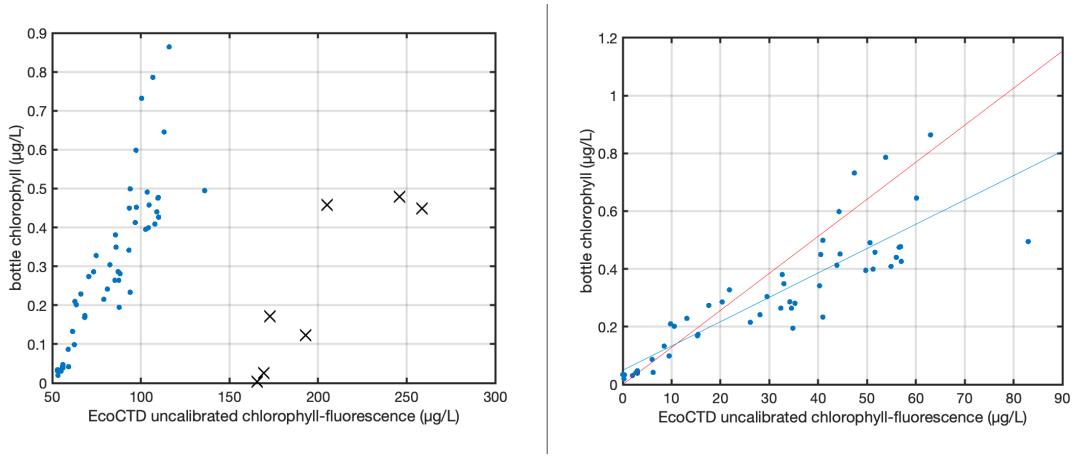

Figure 11: EcoCTD uncalibrated chlorophyll-fluorescence plotted against bottle chlorophyll, including cast 17 (denoted by black X's) (left). EcoCTD uncalibrated chlorophyll-fluorescence plotted against bottle chlorophyll with linear regression line (blue line) and weighted fit (red line)

for all casts except 17 (right). Cast 17 data resulted in outliers due to questionable data quality and was left out of the fits.

3.2.3 Particulate organic carbon (POC) proxies from EcoCTD bb(700) on CTD-Rosette

Cast 17 was excluded due to questionable bio-optical measurements (2 orders of magnitude higher than other casts, despite POC values being within range), and cast 7 was excluded due to questionable bottle POC measurements (Fig. 12, red labels). Note the opposite trend between bb(700) and bottle POC measurements (Fig. 12, #7). This trend was also observed in CTD cp profiles taken by the RBR Maestro (Fig. 16).

EcoCTD bb(700) and corresponding bottle POC was matched up by depth. A line was fit between corrected EcoCTD bb(700) and bottle POC, minimizing the mean square error. The fit was significant ($R_{adj}^2 = 49.9\%$, $F_{1,23} = 24.9$, $P < 0.001$; Fig. 13, Eq. 11).

$$[\text{EcoCTD POC } (\mu\text{mol/L}] = 4559\ [\text{bb}(700)\ (\text{m}^{-1}\text{sr}^{-1})] - 1.75 \qquad (11)$$

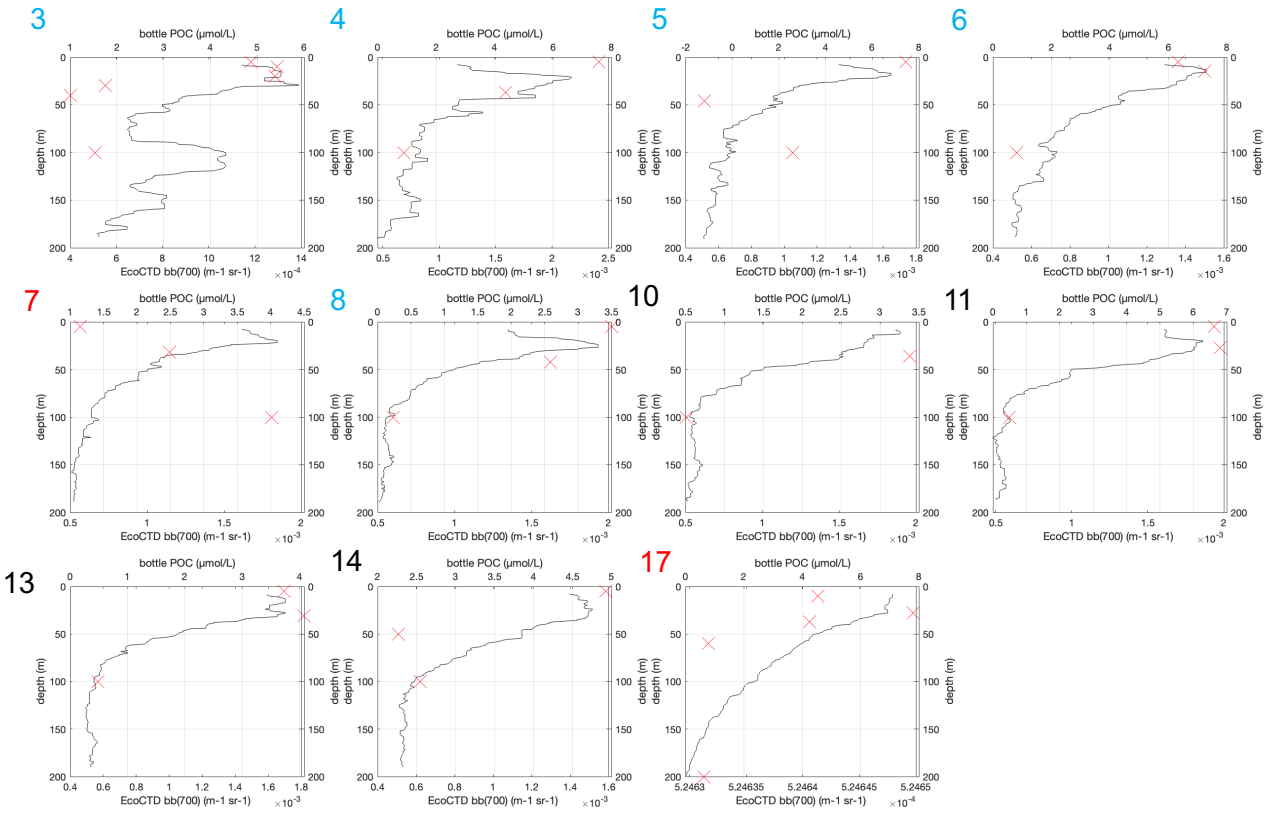

Figure 12: Depth plotted against bottle POC (top x-axis) in red. Depth plotted against EcoCTD bb(700) (bottom x-axis) in black.

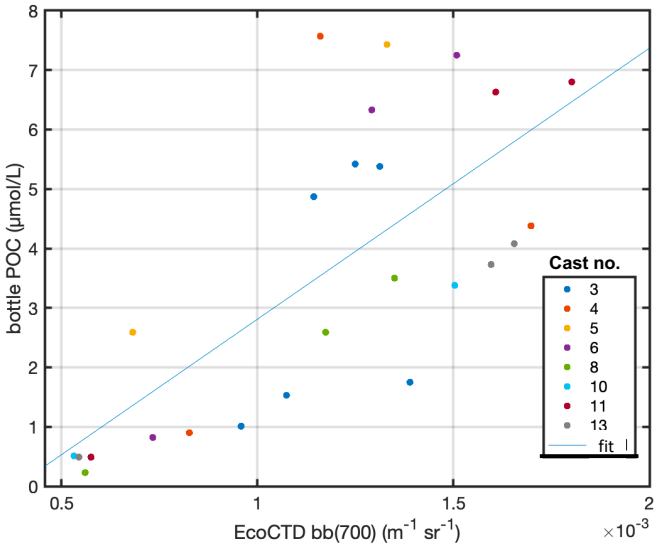

Fig 13: Bottle POC plotted against EcoCTD bb(700). Points colored by cast numbers. Regression line in blue.

3.2.5 RBR Maestro on CTD-Rosette Chl and POC

Raw chlorophyll-fluorescence from the RBR Maestro, which was mounted on the CTD-Rosette, was first corrected by subtracting a "dark count" found by the median of deep values (between 180-200 m). We then fit a line between extracted chlorophyll from bottle samples and chlorophyll-fluorescence taken by on RBR Maestro, forcing the slope to 0. We matched up data by depth. The fit was significant (R_{adj}^2 = 75.4%, $F_{1,75}$ = 695, $P < 0.001$; Fig. 14a, Eq. 12):

$$[\text{calibrated chl-fl } (\mu g/L)] = 0.0059[\text{chl-fl (volts)} - \text{DARK}] \quad (12)$$

$$\text{DARK} = \text{median (chl-fl between 180 m and 200 m)}$$

POC was calibrated by fitting a line between between POC from Niskin bottle samples and beam attenuation from the RBR Maestro. One POC value was thrown away for being significantly below 0 (POC = -1.1 µmol/L) and a second POC value that was close to 0, but negative, was forced to 0 (-0.06 µmol/L). The fit was significant (R_{adj}^2 = 67.1%, $F_{1,47}$ = 99, $P < 0.001$; Fig. 14b, Eq. 13):

$$[\text{POC } (\mu mol/L)] = 16.3[\text{cp } (m^{-1})] - 26.0 \quad (13)$$

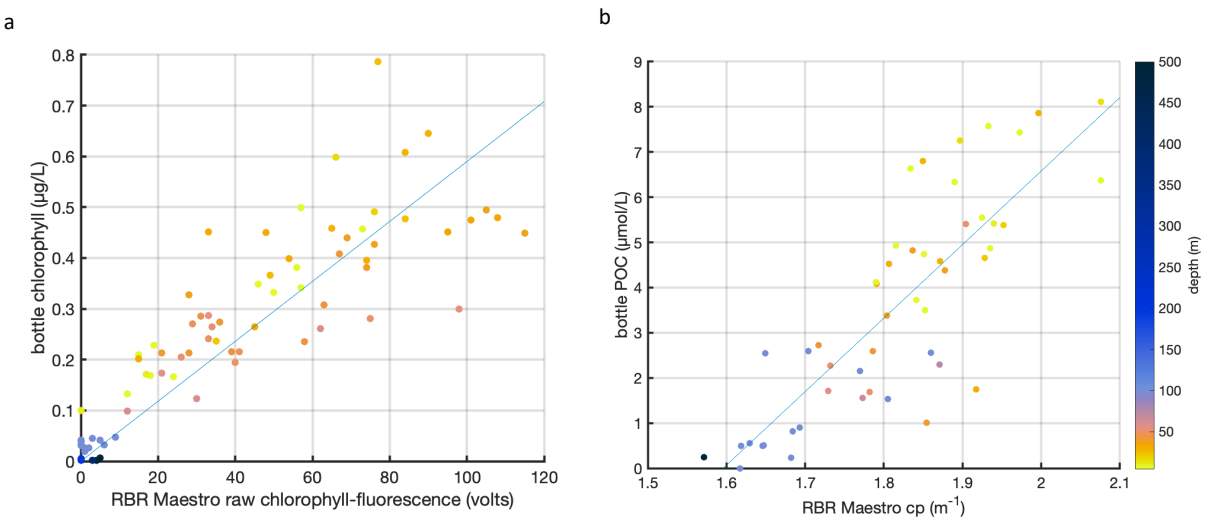

Fig 14: Bottle chlorophyll plotted against raw chlorophyll fluorescence (a). Bottle POC plotted against beam attenuation (cp). Fits in blue. Points colored by depth of measurement.

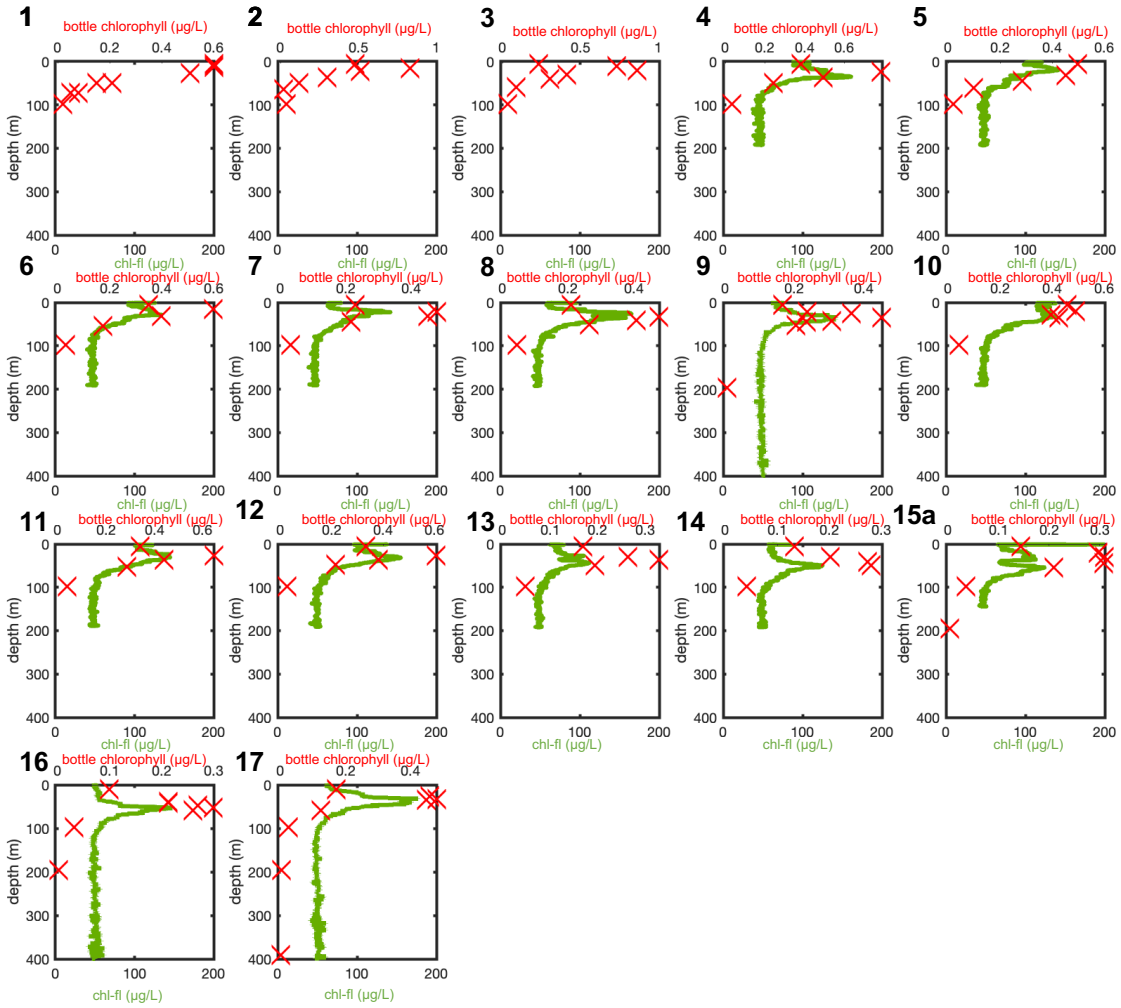

Figure 15: Depth plotted against bottle chlorophyll (top x-axis) in red. Depth plotted against RBR Maestro chl-fl (bottom x-axis) in green.

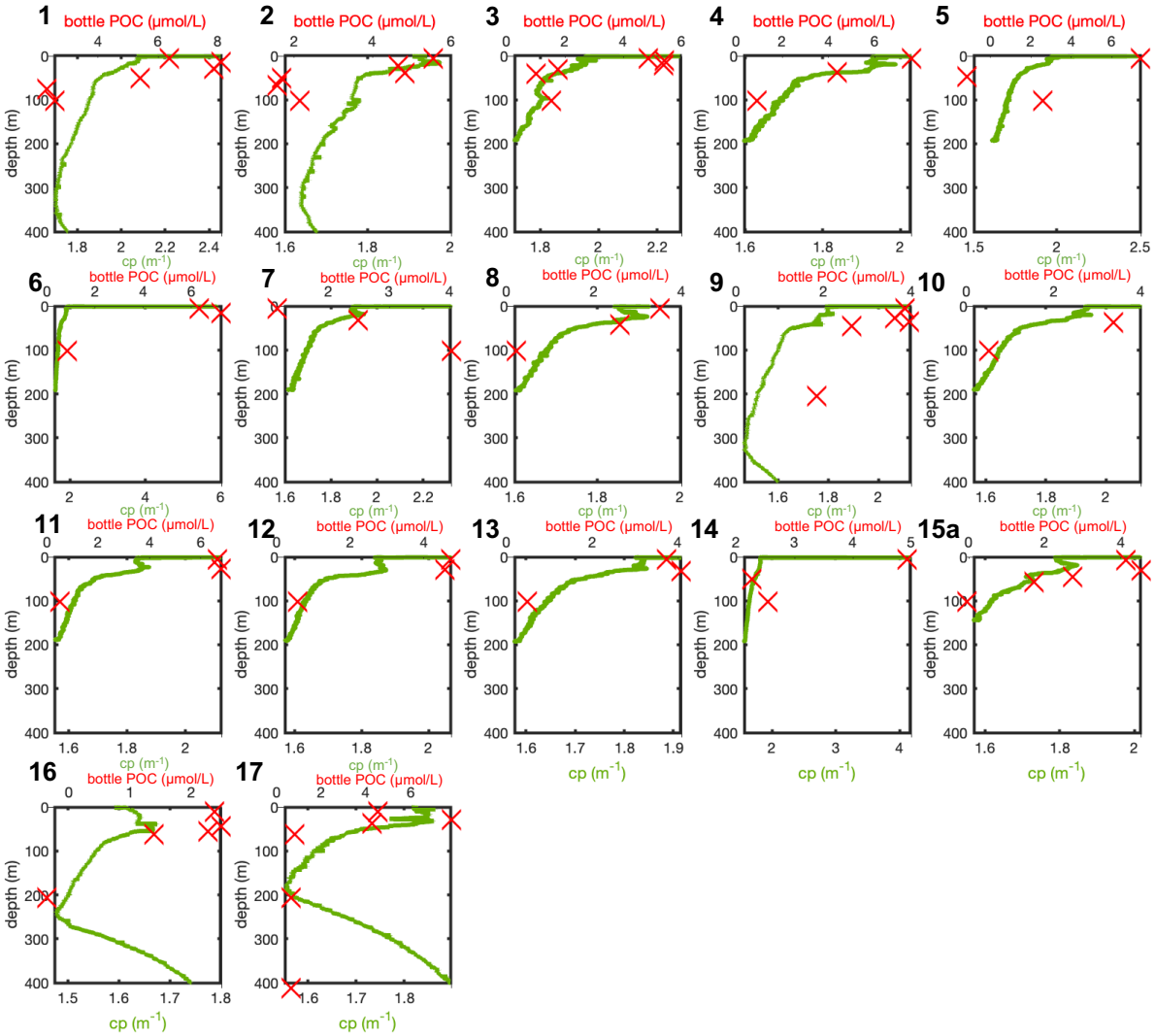

Figure 16: Depth plotted against bottle POC (top x-axis) in red. Depth plotted against RBR Maestro cp(650) (bottom x-axis) in green.

We advise against using cp and POC data from casts 9, 16, and 17 due to questionable cp data.

3.3 Secondary optical proxies (developed based on intercalibration with primary proxy)

3.3.1 Calibrated flow-through Chl-Fl (calibrated from ACS-derived Chl)

Nighttime fluorescence was used to calibrate the Wetlabs chlorophyll fluorometer to avoid the effects of non-photochemical quenching during the day. The fit between ACS-derived

chlorophyll and uncalibrated nighttime chlorophyll-fluorescence was significant (R_{adj}^2 = 79.3%, $F_{1,8837}$ = 3.4e4, $P < 0.001$; Fig. 17, Eq. 14).

$$[\text{calibrated chl-fl (µg/L)}] = 1.72[\text{uncalibrated chl-fl (µg/L)}] + 0.031 \quad (14)$$

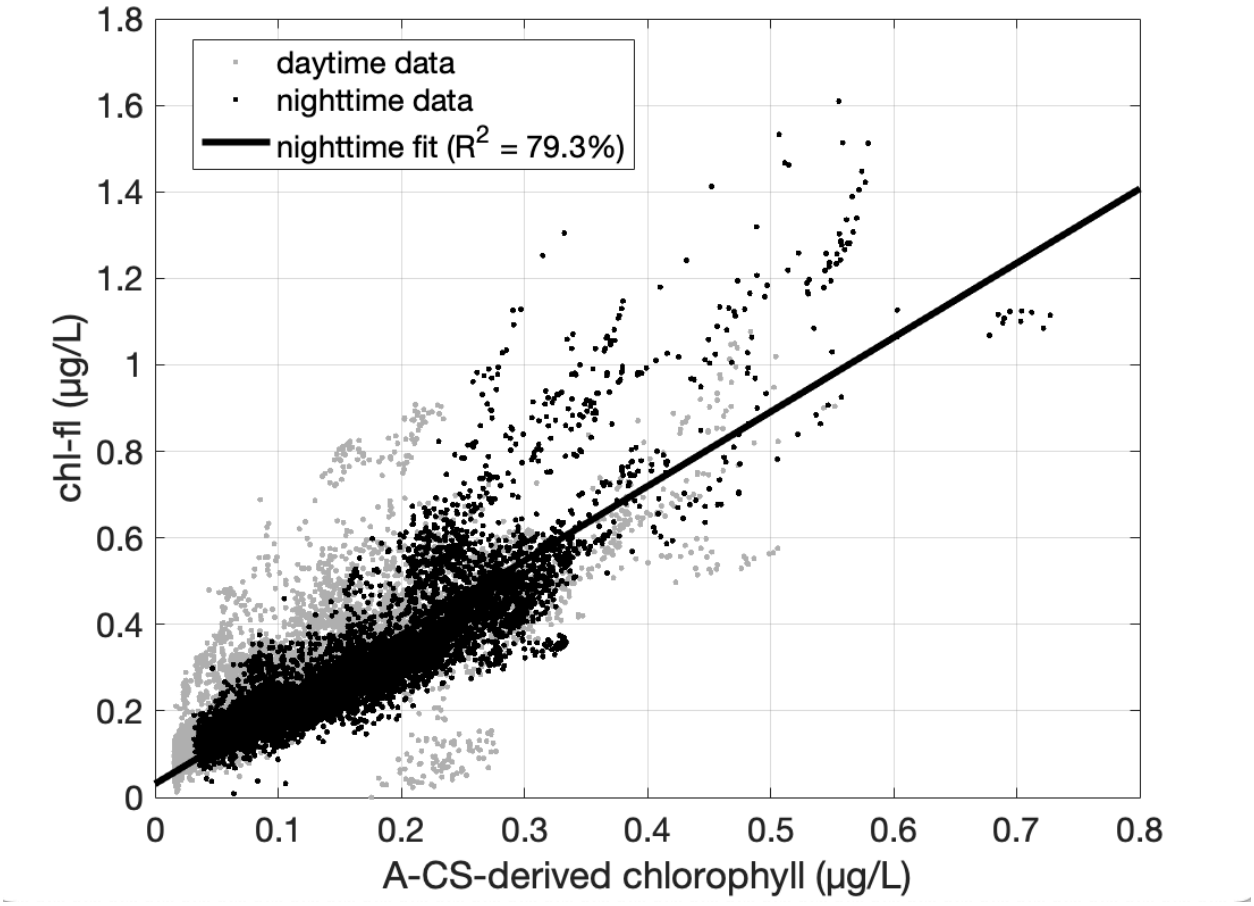

Figure 17: Uncalibrated chlorophyll fluorescence from Wetlabs chlorophyll fluorometer (y-axis) plotted against ACS-derived chlorophyll – a (x-axis). Daytime data shown in gray, and nighttime data shown in black. Nighttime fit shown in black.

3.3.2 Seaglider calibrated Chl-Fl

Seaglider 180 stopped recording data on October 9, 2022 and was left out of the calibrations.

Seagliders 219 and 247 were calibrated by cast #16, and seagliders 220 and 237 were calibrated by cast #17, both taken at the end of the cruise (28-Oct-2022 21:00 and 28-Oct-2022 23:44). The closest Seaglider profile in time to the CTD calibration casts were used for calibration, except for 247 which used the second closest profile in time (closest had data gaps).

Seaglider chl-fl was then calibrated by fitting a line between calibrated chl-fl from the calibration casts (calibrations described in 3.2.5) and uncalibrated Seaglider chl-fl. Data was matched up by density (data not co-located).

The chl-fl fits were significant for all Seagliders: Seaglider 219 (R^2_{adj} = 75.5%, $F_{1,87}$ = 272, P < 0.001, Eq. 15), Seaglider 247 (R^2_{adj} = 93.6%, $F_{1,88}$ = 1300, P < 0.001, Eq. 16), Seaglider 220 (R^2_{adj} = 90.9%, $F_{1,89}$ = 902, P < 0.001, Eq. 17), and Seaglider 237 (R^2_{adj} = 92.3%, $F_{1,92}$ = 1020, P < 0.001, Eq. 18) (Fig 18).

After the calibrations were applied, some values were less than 0, but these were less than the RMSEs of the fit (219: RMSE = 0.076 µg/L, 247: RMSE = 0.041 µg/L, 220: RMSE = 0.052 µg/L, 237: RMSE = 0.048 µg/L) and therefore forced to 0.

Seaglider 219: [calibrated chl-fl (µg/L)] = 0.53 [chl-fl (volts)] + 0.010 (15)

Seaglider 247: [calibrated chl-fl (µg/L)] = 0.53[chl-fl (volts)] – 0.028 (16)

Seaglider 220: [calibrated chl-fl (µg/L)] = 0.46[chl-fl (volts)] – 0.016 (17)

Seaglider 237: [calibrated chl-fl (µg/L)] = 0.50 [chl-fl (volts)] – 0.032 (18)

Seaglider 219 (calibrated by cast #16)

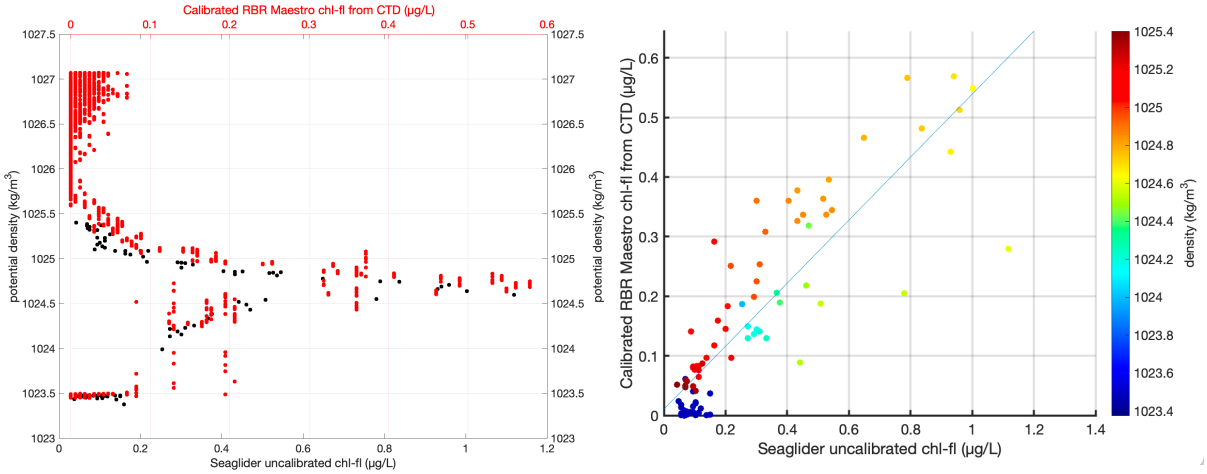

Seaglider 247 (calibrated by cast #16)

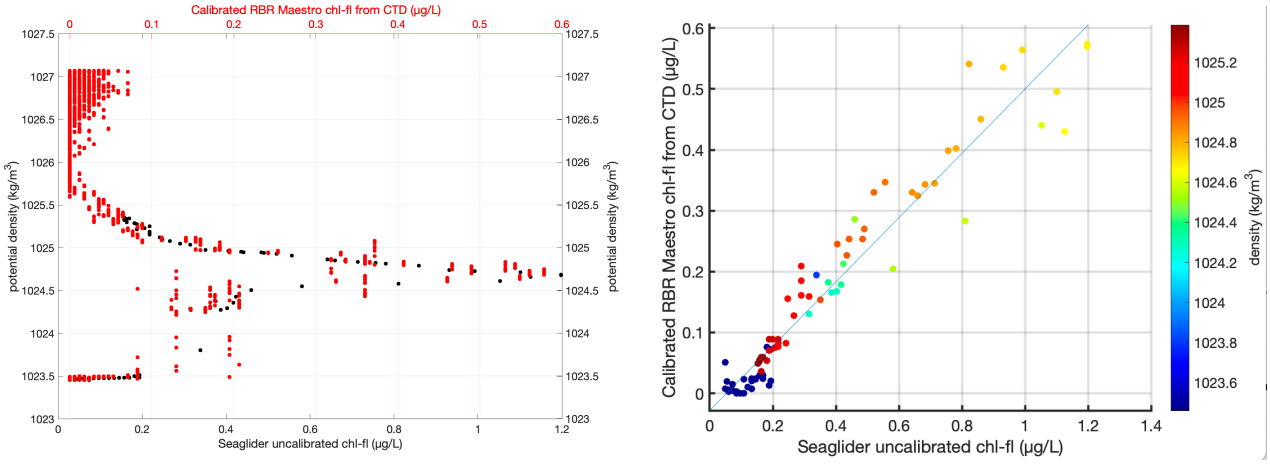

Seaglider 220 (calibrated by cast #17)

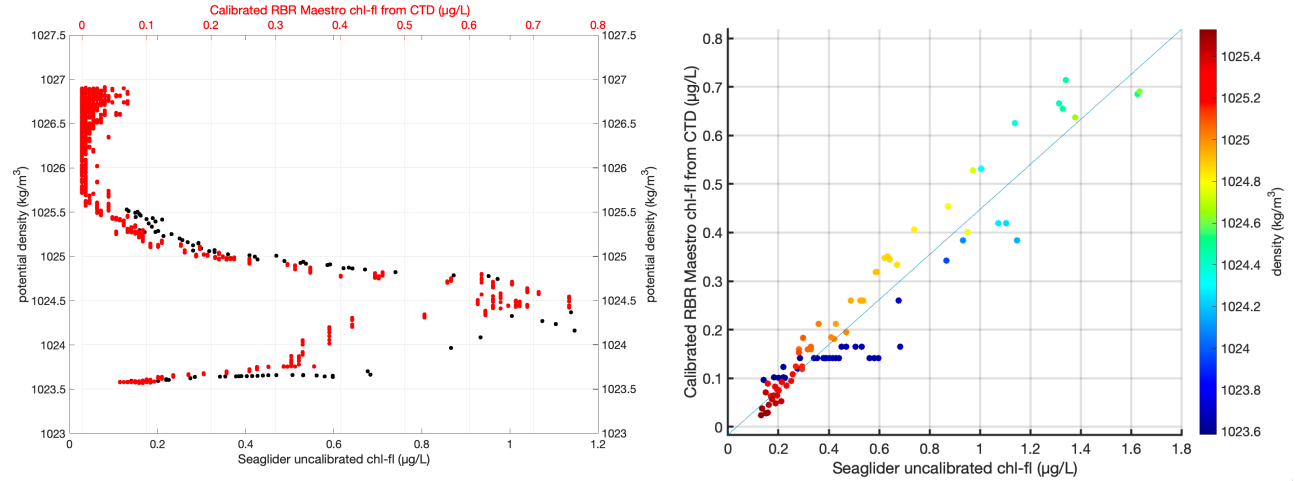

Seaglider 237 (calibrated by cast #17)

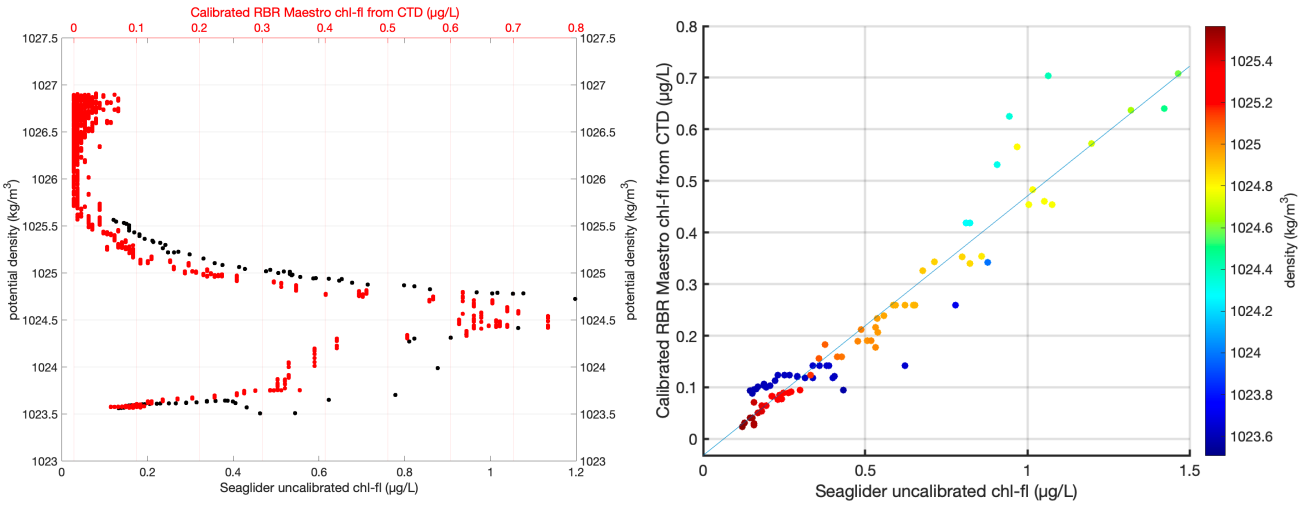

Figure 18: Potential density (kg/m^3) plotted against calibrated RBR Maestro chl-fl (µg/L) in red (top x-axis) and potential density (kg/m^3) plotted against Seaglider uncalibrated chl-fl (µg/L) in black (bottom x-axis) for 4 Saildrones (left plots). Calibrated RBR Maestro chl-fl (µg/L) plotted

against Seaglider uncalibrated chl-fl (µg/L) at same potential density (right plots). Points in right plot colored by potential density, and calibration fits (Eqs. 15-18) in blue.

3.3.3 Seaglider calibrated POC

Beam attenuation data from the calibration casts (POC proxy from calibration casts) were questionable (Section 3.2.5, Fig. 16), so could not be used for Seaglider POC calibrations. Instead, bottle POC samples from the calibration casts were used to calibrate Seaglider POC. Data was matched up by density, and a line was fit between bottle POC samples and Seaglider bb(700). In V3, a more sophisticated intercalibration will be investigated using nearby EcoCTD to-yoed profiles.

$$\text{Seaglider 219: [POC (µmol/L)]} = 8845\ [bb(700)\ (m^{-1}sr^{-1})\ ] - 0.51 \quad (19)$$

$$\text{Seaglider 247: [POC (µmol/L)]} = 4455\ [bb(700)\ (m^{-1}sr^{-1})\ ] - 2.00 \quad (20)$$

$$\text{Seaglider 220: [POC (µmol/L)]} = 1461\ [bb(700)\ (m^{-1}sr^{-1})\ ] + 0.46 \quad (21)$$

$$\text{Seaglider 237: [POC (µmol/L)]} = 928\ [bb(700)\ (m^{-1}sr^{-1})\ ] + 1.13 \quad (22)$$

Seaglider 219 (calibrated by cast #16)

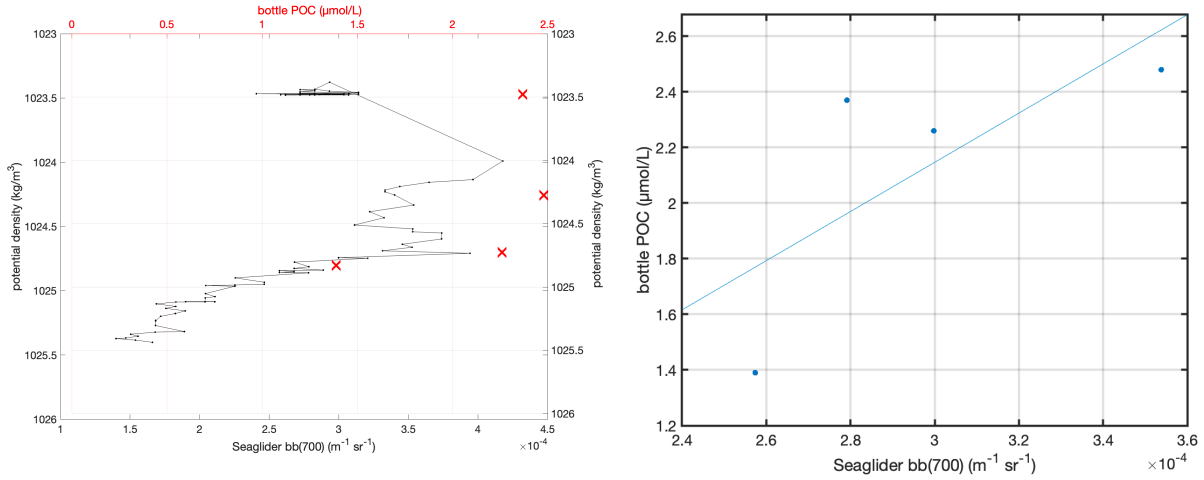

Seaglider 247 (calibrated by cast #16)

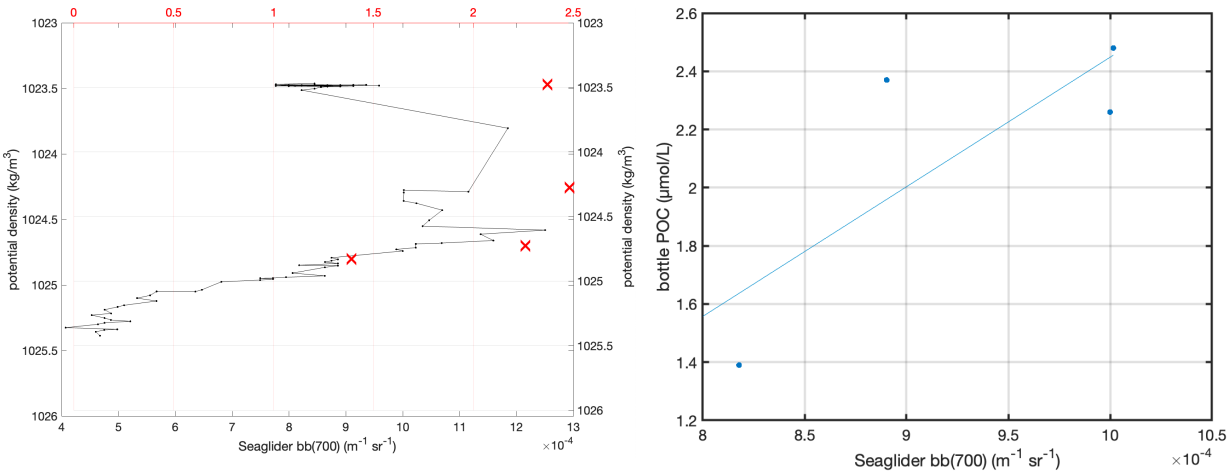

Seaglider 220 (calibrated by cast #17)

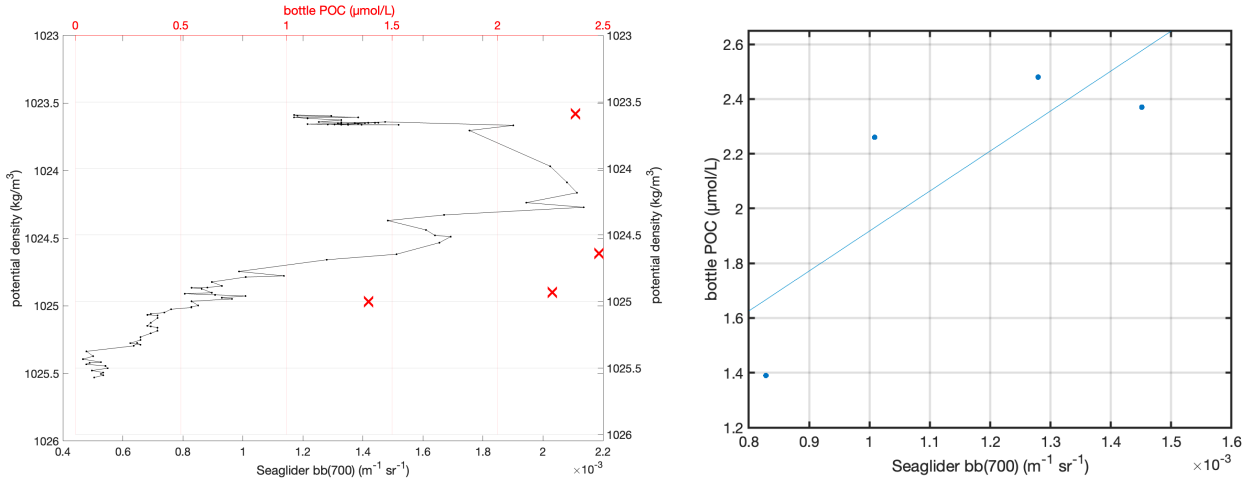

Seaglider 237 (calibrated by cast #17)

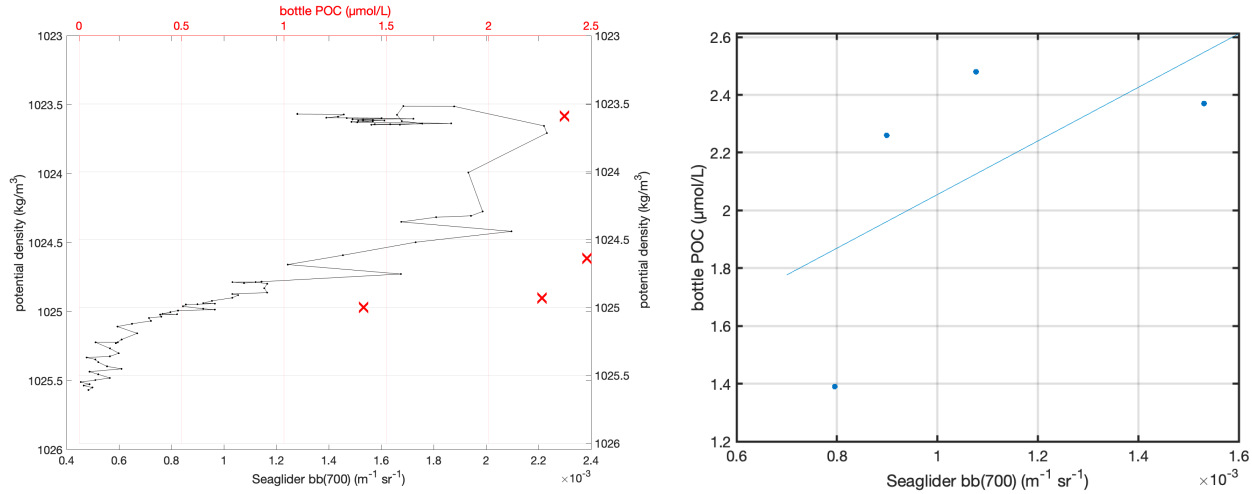

Figure 18: Potential density (kg/m^3) plotted against calibrated against bottle POC (µmol/L) in red (top x-axis) and potential density (kg/m^3) plotted against Seaglider uncalibrated bb(700) (m-1 sr-1) in black (bottom x-axis) for 4 Seagliders (left plots). Bottle POC (y-axis) plotted against

Seaglider uncalibrated bb(700) (m-1 sr-1) at same potential density (right plots). Calibration fits (Eqs. 19-22) in blue.

3.3.4 Saildrone calibrated Chl-Fl

Saildrone chl-fl was first multiplied by 1e6 to convert kg/m^3 to µg/L.

Chl-fl from the Saildrone was matched up with ship-based chlorophyll (ACS-based proxy) measured at the same time and within 1 km.

Saildrone 1087, 1085, and 1026 chl-fl had strong linear relationships with ship-based chlorophyll (1087: R^2_{adj} = 77.2%, $F_{1,350}$ = 1190, $P < 0.001$, Eq. 23; 1085: R^2_{adj} = 73.9%, $F_{1,282}$ = 802, $P < 0.001$, Eq. 24; 1026: (R^2_{adj} = 79.9%, $F_{1,520}$ = 2070, $P < 0.001$, Eq. 26). Chl-fl from Saildrone 1048 had poor data quality (Fig. 19). The listed calibration (Eq. 25) is an average of the slopes and intercepts of the other three calibrations. We advise against using this data.

Saildrone 1087: [calibrated chl-fl (µg/L)] = 0.26 [chl-fl (volts)] + 0.12 (23)

Saildrone 1085: [calibrated chl-fl (µg/L)] = 0.27[chl-fl (volts)] + 0.10 (24)

*** Saildrone 1048: [calibrated chl-fl (µg/L)] = 0.27 [chl-fl (volts)] + 0.12 (25)

Saildrone 1026: [calibrated chl-fl (µg/L)] = 0.28 [chl-fl (volts)] + 0.12 (26)

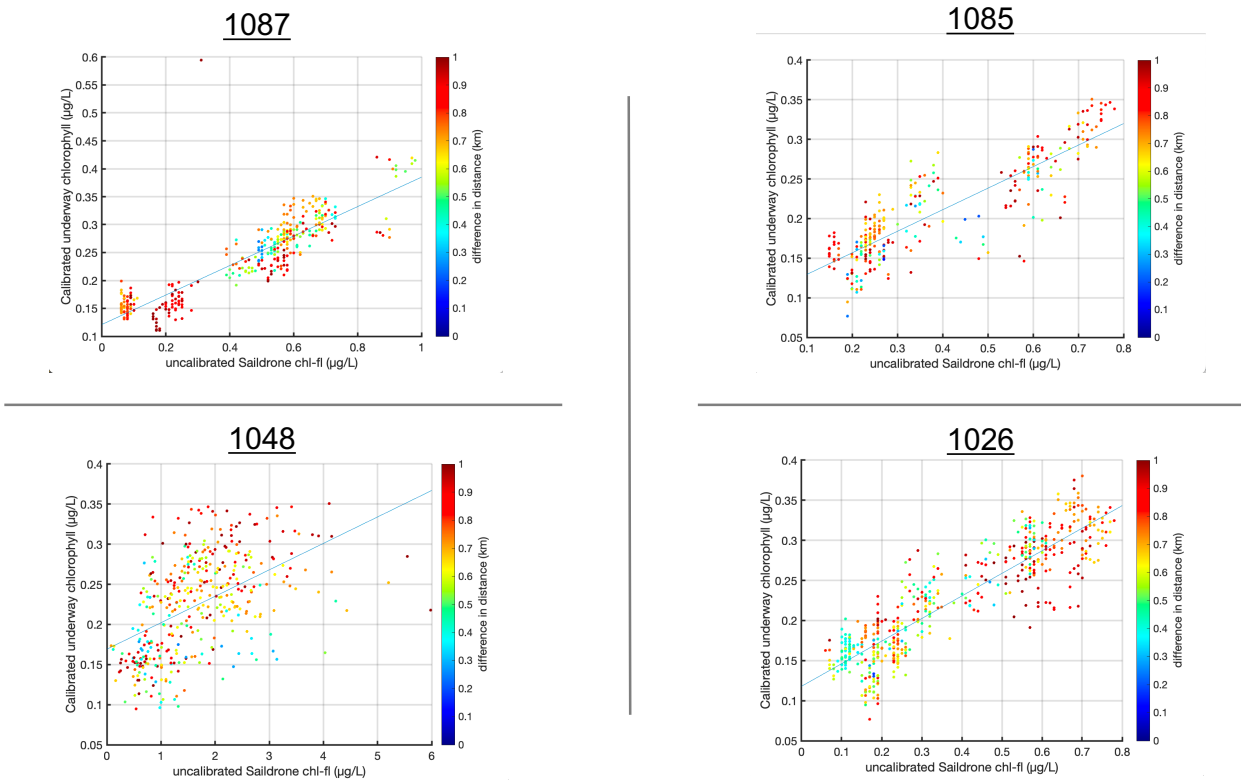

Figure 19: Calibrated underway chlorophyll (µg/L) plotted against uncalibrated Saildrone chl-fl (µg/L) for all 4 Saildrones. Points colored by the difference in distance between the ship and the Saildrone. Saildrones 1087, 1085, and 1026 had strong correlations with underway chlorophyll, but Saildrone 1048 did not do to poor Chl-fl data quality.

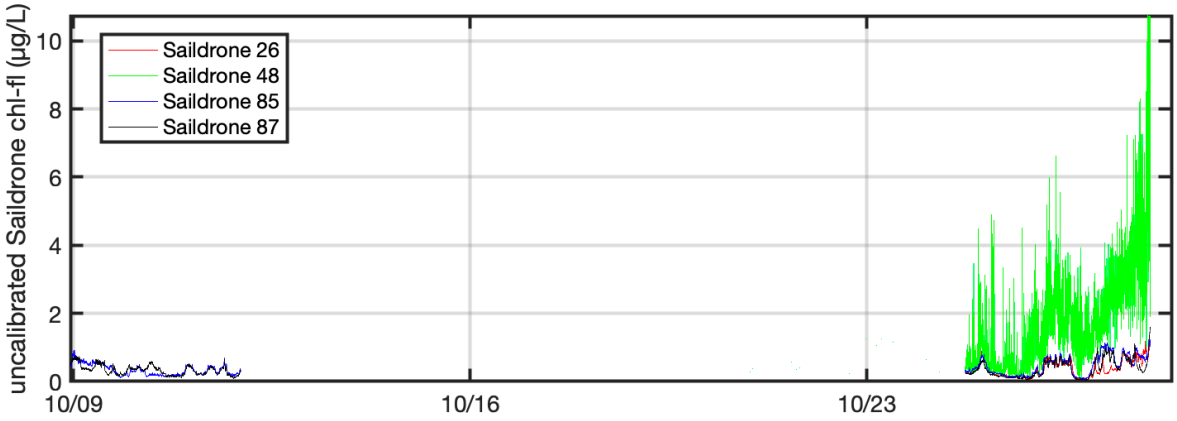

Figure 20: Uncalibrated Saildrone Chl-fl plotted against time. Saildrone 1048 (green) had poor data quality.

3.3.5 Saildrone calibrated POC

Bb(650) from the Saildrone was matched up with ship-based POC (ACS-based proxy) measured at the same time and within 1 km. Spikes were removed from backscatter data with a 5-point (5 minute) median filter.

Saildrone 1087 and 1085 bb(650) and ship-based POC had significant fits (1087: R^2_{adj} = 33.7%, $F_{1,351}$ = 180, $P < 0.001$, Eq. 27; 1085: R^2_{adj} = 32.4%, $F_{1,283}$ = 137, $P < 0.001$, Eq. 28).

Saildrone 1048 and 1026 bb(650) had stronger relationships with Saildrone 1087 calibrated POC (1048: R^2_{adj} = 86.2%, $F_{1,804}$ = 5010, $P < 0.001$, Eq. 29; 1026: R^2_{adj} = 91.8%, $F_{1,283}$ = 3390, $P < 0.001$, Eq. 30) than ship-based POC (1048: R^2_{adj} = 10.8%, $F_{1,392}$ = 48.5, $P < 0.001$; 1026: R^2_{adj} = 7.5%, $F_{1,521}$ = 43.2, $P < 0.001$), and therefore the former fit was used for calibration.

Saildrone 1087: [POC (µmol/L)] = 3537 [bb(650) ($m^{-1}sr^{-1}$)] – 0.41 (27)

Saildrone 1085: [POC (µmol/L)] = 6126 [bb(650) ($m^{-1}sr^{-1}$)] – 5.76 (28)

Saildrone 1048: [POC (µmol/L)] = 3804 [bb(650) ($m^{-1}sr^{-1}$)] - 0.33 (29)

Saildrone 1026: [POC (µmol/L)] = 3533 [bb(650) ($m^{-1}sr^{-1}$)] – 0.06 (30)

1087 *(intercalibration with ship)*

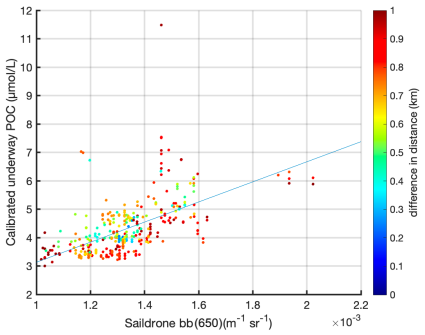

1085 *(intercalibration with ship)*

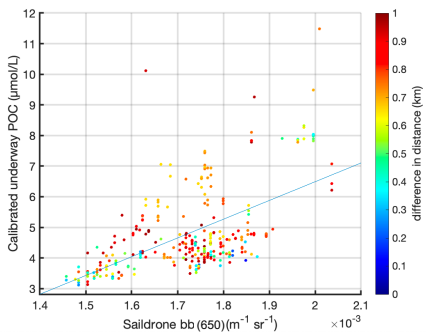

1048 *(intercalibration with Saildrone 1087)*

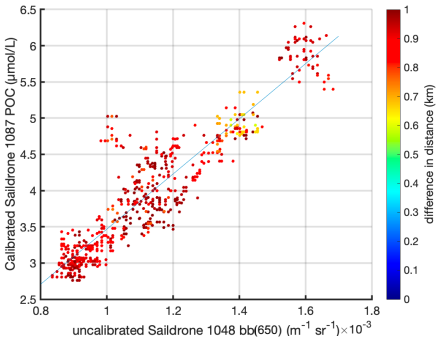

1026 *(intercalibration with Saildrone 1087)*

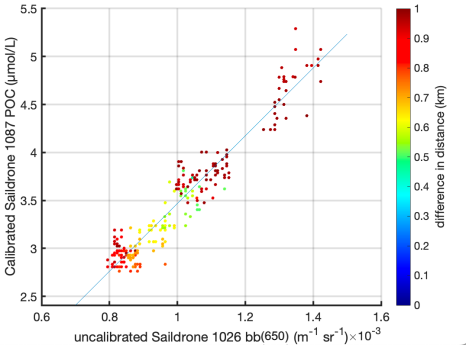

Figure 21: Calibrated underway POC (µmol/L) plotted against uncalibrated Saildrone bb(650) (m-1 sr-1) for all 4 Saildrones. Points colored by the difference in distance between the ship and the Saildrone. Saildrones 1087 and 1085 had significant correlations with underway POC, but Saildrones 1048 and 1026 did not. However, Saildrones 1048 and 1026 bb(650) had strong correlations with Saildrone 1087 POC, so this relationship was used for calibration.

3.3.6 Waveglider POC

A linear fit between bb(700) and flow-through POC (R^2_{adj} = 88.7%, $F_{1,29}$ = 236, $P < 0.001$; Eq. 31; Fig. 22) was used as the calibration curve for bb-based POC. Match-ups were within 2 km and 1 minute. Negative points (≥ -1 µmol/L, 1.9% of the data) were forced to 0.

$$[\text{POC (µmol/L)}] = 7043\ [\text{bb(700) (m}^{-1}\text{sr}^{-1})] - 5.97 \quad (31)$$

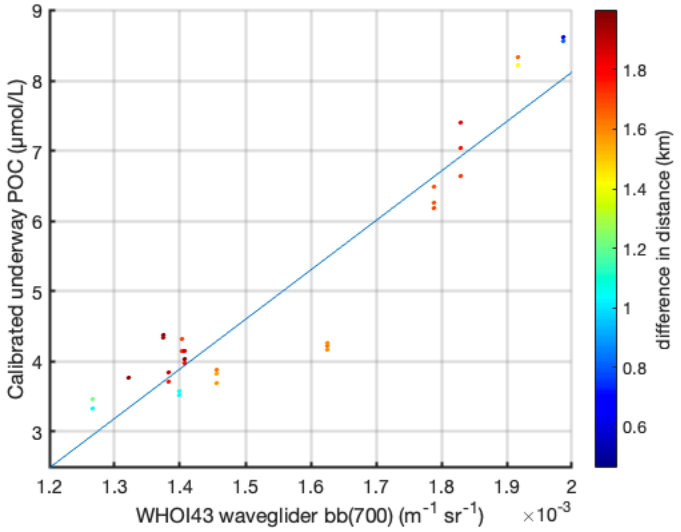

Figure 22: Calibrated underway POC from cp plotted against waveglider bb(700). Fits in blue. Points colored by distance between match-ups in kilometers.

A 6-point (30 second) median filtered was applied to bb-based POC data. A linear fit between cp and bb-based POC from the Waveglider (R^2_{adj} = 79.4%, $F_{1,29}$ = 50,400, $P < 0.001$; Eq. 32; Fig. 23) was used as the calibration curve for the cp-based POC proxy:

$$\text{POC (µmol/L)}] = 59.8\ [\text{cp (m}^{-1})] - 381 \quad (32)$$

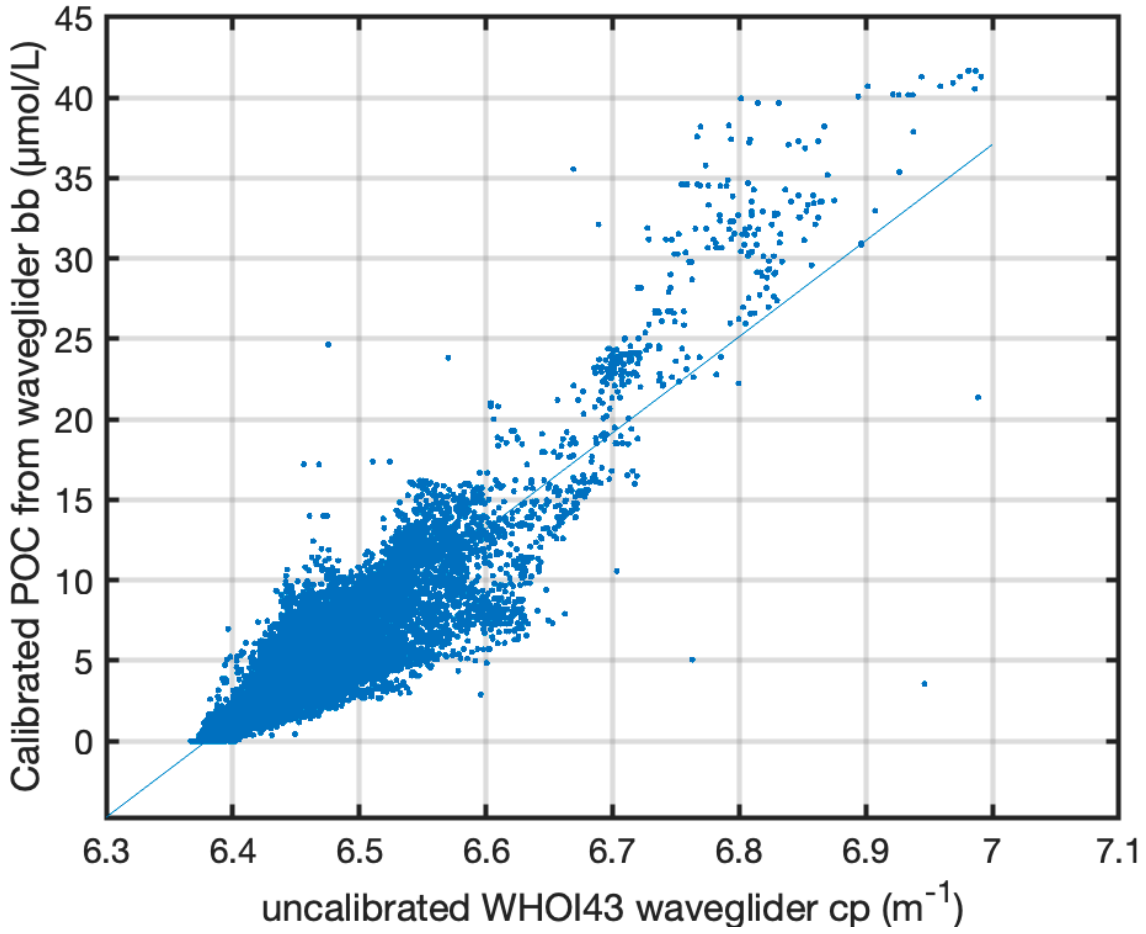

Figure 23: bb-based POC plotted against waveglider cp. Linear fit in blue.

Negative values (≥ -1 µmol/L, 1.4% of the data) were forced to 0.

Acknowledgements

We thank Emmanuel Boss and his lab for their equipment, software, and training that helped create the flow-through optics dataset.

Citations

Behrenfeld, & Boss, E. (2006). Beam attenuation and chlorophyll concentration as alternative optical indices of phytoplankton biomass. Journal of Marine Research, 64. https://doi.org/10.1357/002224006778189563

Boss, E., and Pegau, S.W., "Relationship of light scattering at an angle in the backward direction to the backscattering coefficient," Appl. Opt. 40, 5503-5507 (2001)

Chase, A., Boss, E., Zaneveld, R., Bricaud, A., Claustre, H., Ras, J., Dall'Olmo, G. and

Westberry, T.K., 2013. Decomposition of in situ particulate absorption spectra. Methods in Oceanography, 7, pp.110-124.

Dall'Olmo G., R. J. W. Brewin, F. Nencioli, E. Organelli, I. Lefering, D. McKee, R. Röttgers, C. Mitchell, E. Boss, A. Bricaud, and G. Tilstone, 2017: Determination of the absorption coefficient of chromophoric dissolved organic matter from underway spectrophotometry. Optics Express, 25(24): A1079-A1095. doi:10.1364/OE.25.0A1079

Farrar, T., et al. (2020), S-MODE: The Sub-Mesoscale Ocean Dynamics Experiment, 3533-3536, doi:10.1109/IGARSS39084.2020.9323112.

IOCCG Protocol Series (2019). Inherent Optical Property Measurements and Protocols: Best Practices for the Collection and Processing of Ship-Based Underway Flow-Through Optical Data. Boss, E., Haëntjens, N., Ackleson, S.G., Balch, B., Chase, A., Dall'Olmo, G., Freeman, S., Liu, Y., Loftin, J., Neary, W., Nelson, N., Novak, M., Slade, W., Proctor, C., Tortell, P., and Westberry. T. IOCCG Ocean Optics and Biogeochemistry Protocols for Satellite Ocean Colour Sensor Validation, Volume 4.0, edited by A. R. Neeley and A. Mannino, IOCCG, Dartmouth, NS, Canada. http://dx.doi.org/10.25607/OBP-664

Lynn, R. J., S. J. Bograd, T. K. Chereskin, and A. Huyer, Seasonal renewal of the California Current: The spring transition off California, J. Geophys. Res., 108(C8), 3279, doi:10.1029/2003JC001787, 2003.

McDougall, T.J. and P.M. Barker, 2011: Getting started with TEOS-10 and the Gibbs Seawater (GSW) Oceanographic Toolbox, 28pp., SCOR/IAPSO WG127, ISBN 978-0-646-55621-5.

Roesler, C. S., & Barnard, A. H. (2013). Optical proxy for phytoplankton biomass in the absence of photophysiology: Rethinking the absorption line height. Methods in Oceanography, 7, 79-94.

Slade, W. H., E. Boss, G. Dall'Olmo, M. R. Langner, J. Loftin, M. J. Behrenfeld, C. Roesler, and T. K. Westberry. (2010). Underway and Moored Methods for Improving Accuracy in Measurement of Spectral Particulate Absorption and Attenuation. J. Atmos. Oceanic Technol., 27, 1733–1746, https://doi.org/10.1175/2010JTECHO755.1.

Zhang, X., Hu, L., and He, M.X. (2009), Scattering by pure seawater: Effect of salinity, Optics Express, Vol. 17, No. 7, 5698-5710